1 About clusters

Although we usually do not realize it, clusters belong to our everyday life. They have been exploited practically in many situations without people being aware of the underlying details. The tailoring of fine dispersed pieces of material (clusters !) inside bulk has, for example, been turned to an art by craft-workers for centuries. Already the Romans knew, empirically, how to play with the size of dispersed particles in a glass to produce various shining colors. Depending on the size of the gold inclusions, a glass could thus exhibit red as well as yellow reflections, for an example see [KV93]. In a different domain, photography also represents a typical application of cluster physics. Depending on the size of the AgBr clusters deposited on the film, they will more or less quickly and finely respond to light and thus perpetuate the properties of the produced image. Early photographers of the nineteenth century quickly realized and controlled such physical behaviors. Still, even at that time, clusters were not considered as objects of scientific studies, even not recognized as specific objects. The work of Mie at the turn of the twentieth century probably constitutes one of the earliest speculations on the existence and specificity of metal clusters — or rather, because the word "cluster" did not exist in this context at that time, of "small particles" [Mie08]. The question raised by Mie concerned the response of small metal particles to light, and how this response might depend on the size of the considered particle. Let us quote Mie: "Because gold atoms surely differ in their optical properties from small gold spheres", it would "probably be very interesting to study the absorption of solutions with the smallest submicroscopical particles; thus, in a way, one could investigate by optical means how gold particles are composed of atoms". A non negligible part of today's investigations on clusters relies on, or is very close to, Mie's intuition. As we shall see throughout this book, light represents a particularly useful means for the investigation of both structure and dynamics of clusters. And the response of clusters to light is indeed extremely sensitive to their properties. The beautiful achievements of Roman and later glass makers precisely reflect such properties. And photography, as well, is an art dealing with light.

The inspiring intuition of Mie did not suffice to promote cluster science to the status of a well recognized field of physics. Indeed the times of the early twentieth century were busy with the identification and analysis of "elementary" constituents of matter and only simple molecules seemed in reach of understanding in the mid century, or alternatively the other extreme, namely the problem of bulk material, of course with other techniques than the ones used in atomic physics. Modern cluster physics, as we know it today, only appeared in the last quarter of the twentieth century with the possibility of producing free clusters and tracking such small particles with several, still developing, techniques. This allowed the initiation of studies on clusters as such, which was an important step for the field. Indeed, embedded

Introduction to cluster dynamics. Paul-Gerhard Reinhard, Eric Suraud

ISBN: 3-527-40345-0

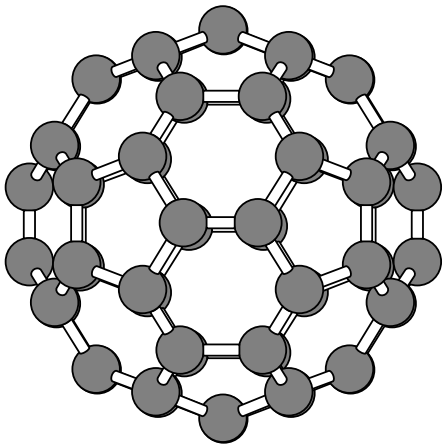

Figure 1.1: Ionic structure of the famous C_{60} cluster. The 60 atoms are arranged as 12 pentagons and 20 hexagons yielding a truncated icosahedron. That shape consists in 12 vertices bound together by 20 equilateral (and equal) triangles. At each vertex of the icosahedron, 5 triangles meet. Truncating these vertices by a plane, leads to the pentagonal faces. The total number of vertices becomes 60. For this C_{60}, 120 symmetry operations can be identified. And this high degree of symmetry has long been used by artists, the actual name of "Buckminster fullerenes" going back to the architect Richard Buckminster Fuller, renowned for his geodesic domes based on pentagons and hexagons.

clusters (as the fine gold particles in Roman glasses), or clusters deposited on surfaces, were experimentally accessible since long and of course the subject of numerous studies. But these rarely concentrated on the clusters, independently from the matrix or substrate. The case was more or less appended to surface or material science and did not constitute a true independent field. The capability of producing free clusters from dedicated sources, allowed the true starting of cluster science on a systematic basis. One of the startup events was the identification of C_{60} clusters, the famous fullerenes [YPC$^+$87, Kro87], with their remarkable geometry shown in Figure 1.1. At about the same time, free metal clusters had been produced and investigated, see e.g. [KCdH$^+$84]. The many original results obtained from then on for metal clusters, carbon clusters and, increasingly, other materials, established cluster physics as an independent, although cross-disciplinary, field among the well defined branches of physics and chemistry. Of course the production and analysis of free clusters gave new impetus to activities on deposited or embedded clusters as well. At the same time, amazing developments in the nanoscopic analysis of surfaces opened new views and much refined analysis of supported clusters. An example is given in Figure 1.2 showing in detail Ag nano-clusters sitting on a HOPG surface. As we will see, the combination of these quickly developing methods of nano-analysis with nano-particles, called clusters, constitutes a powerful tool for fundamental and applied physics.

The physics and chemistry of clusters, with its many facets covering free as well as embedded or deposited clusters, addresses an impressive set of problems, ranging from fundamental to applied ones. In all that, clusters are a species of their own asking for specific understanding of their properties. Although molecular and solid state physics, as well as chemistry or nuclear physics, do add helpful aspects, clusters belong to none of these fields and thus require devoted methods, both at the experimental and theoretical levels. A specific feature is, e.g., that cluster size can be varied systematically between atoms and bulk: they are, so to say, "scalable" objects. Clusters thus play an essential role from a fundamental physical point of view. They do represent an exceptional opportunity for testing the many-body problem, which is a generic quantum mechanical task and lies at the heart of the understanding of most complex systems. Bear in mind that solid state physics deals with virtually infinite, although

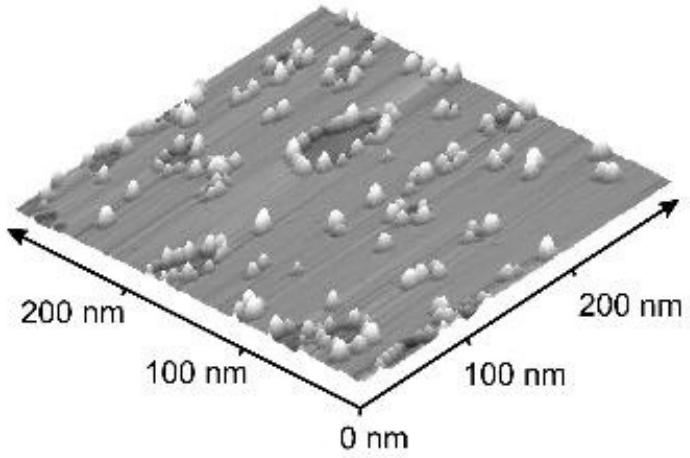

Figure 1.2: Topography of silver nanoparticles deposited on highly oriented pyrolytic graphite (HOPG), recorded with an *in situ* scanning tunneling microscope (STM). From [LMP$^+$00].

symmetric, samples while in molecular or nuclear physics the systems never contain more than a few hundreds of constituents. Clusters bridge the gap. But the interest in them is not purely fundamental. As outlined above, clusters play a role in many practical situations like photography or artwork. More precisely, they have applications in many fields of science as, e.g., astrophysics, chemistry or material science. For example, clusters seem to play an important role in the formation mechanisms and the properties of cosmic dust [CTB89]. Carbon clusters are also expected to be present in the interstellar medium. The most striking property of clusters for applications in chemistry is their size. Indeed, because clusters may be quite small, but not too small, they can exhibit a large and tunable surface to volume ratio. They may thus provide ideal catalysts and play a crucial role in reaction kinetics [SAH$^+$99]. A typical example of application here is photography. In material science, the discovery of fullerenes and carbon nanotubes opened the way to the design of new materials [Kai01]. This breakthrough renewed chemistry and physics of carbon to such a level that this field is almost becoming independent from the mother field of cluster physics, probably in part because of its many industrial applications.

Cluster physics with its many achievements now belongs to one of the most active fields in physics, and offers, through related domains like the physics of nanotubes or fullerenes, one of the fastest developing areas in applied as well as in fundamental science. It is close to impossible to cover in a single book all the topics related to cluster physics. We shall thus focus here on one important aspect of the field: cluster dynamics. As in atomic and molecular physics, detailed studies on the dynamics of quantum many-body systems were boosted by the rapid progress of laser technology and the possibility of studying electronic motion at the femtosecond (fs) level. Clusters add to these studies the variability of sizes, as discussed

above. Of course, the field of cluster science is so recent that we shall devote a large part of the book to the principle methods of cluster physics, experimental ones (in Chapter 2) as well as theoretical ones (in Chapter 3). Before that, we are going discuss in this chapter here the nature of clusters in relation to more established objects such as atoms and molecules, on the one side, and bulk, on the other side. Not surprisingly, we shall see that size turns out to be a key quantity, influencing many cluster properties. And we shall see that clusters are more than just big molecules or "small" pieces of bulk. They are indeed objects of their own, and cluster physics thus has to combine expertise from various fields of physics and chemistry into an excitingly new area of research.

1.1 Atoms, molecules and solids

Before considering clusters made of atoms, it is useful to briefly summarize what we need to know on the more "traditional" systems such as atoms, molecules and solids. Clusters range between these extremes and we shall see that understanding binding mechanisms between atoms or inside bulk provides the necessary keys to understand binding of clusters. Starting point is the atoms, then we discuss their combination in terms of molecules and in the infinite limit in terms of solids. We can then address clusters. For all species, we give here a brief overview with bias on the electronic structure, mostly at a qualitative level. For more thorough discussions, we refer the reader to standard textbooks of atomic, molecular, chemical physics or solid-state physics as cited at the relevant places.

1.1.1 Atoms

1.1.1.1 Qualitative aspects

Atoms consist of a central nucleus and a neutralizing electronic cloud. The atomic number Z labels the charge of the nucleus which is the number of protons inside the nucleus. The other constituents are the neutrons which, however, play a negligible role for the electronic problem, at least at the level we are interested in. For our purpose, we can safely reduce the effect of the nucleus to that of a point charge Ze (thus neglecting hyper-fine structure as effects of finite size and magnetic coupling [YH96]). Electrons are then supposed to feel only the Coulomb field of the (point-) nucleus. At the level of the fine structure, there are the relativistic effects on the electrons as spin-orbit splitting and Breit interaction [Wei78]. These are, in fact, crucial for heavy elements or when going for quantitative details of bonding. Nonetheless, we neglect fine structure in the discussions of this book to keep the presentation simple.

What remains is the non-relativistic many-electron problem in the central field of the nucleus. It is well known that the electrons arrange themselves in shells around the nucleus. The quantitative understanding of the arrangement of these shells is a non-trivial problem, except for the case of the hydrogen atom where the problem reduces to one single electron in a central field. The case of many-electron atoms quickly becomes complex because of the two-body coulomb interactions between electrons. It is usually treated in a mean-field approximation where each electron is supposed to feel the net effect of all other electrons as one common central mean field. This allows one to sort electrons in shells denoted by their orbital angu-

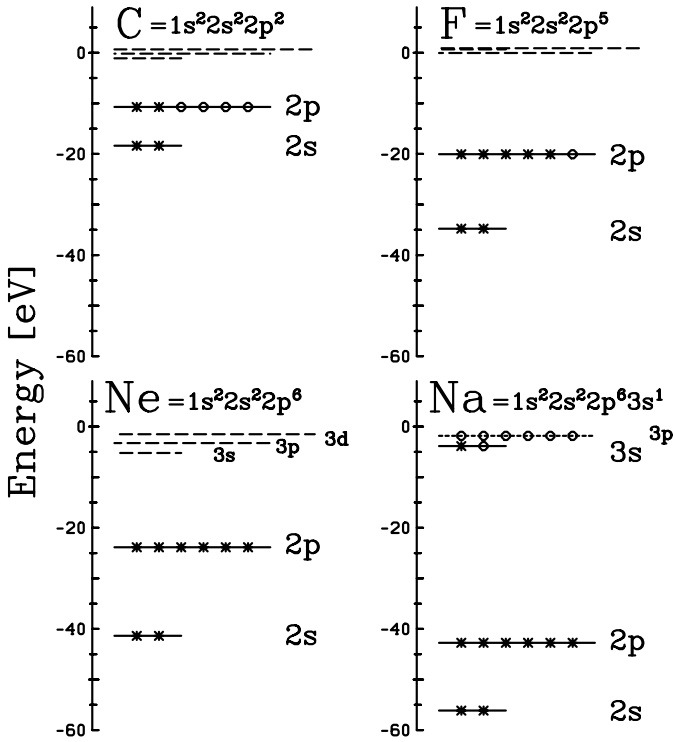

Figure 1.3: Level schemes for the C, F, Ne, and Na atoms. Open circles and/or dashed lines indicate empty states, crosses occupied states. The same energy scale is used for all 4 atoms for better comparison. The spectroscopic notation is given for each atom.

lar momentum and sorted according to increasing single-electron energy. Without entering details which can be found elsewhere (see [Wei78] and Appendix B), we want to remind the basic "Aufbau" principle of electronic shells. Let's imagine that we fill the atom successively, electron by electron. The first electron will feel only the nuclear attraction as a pure Coulomb field. But already the second electron experiences both the nuclear attraction and the repulsion due to the first electron. Both electrons will stabilize to form the most deeply lying electronic level, the $1s$ shell, filled with these two electrons and distinguished by spin up or down. The third electron has to fight the conflicting influence of the attracting nucleus and the two repelling $1s$ electrons. It will feel a screened nuclear charge $(Z-2)|e|$ and form, together with the next electron to come, the $2s$ electronic shell. Because the nuclear charge is screened, the $2s$ shell is much less bound than the $1s$ shell of the pure nuclear field. Mind also that the Pauli principle does hinder these $2s$ electrons to approach the nucleus in the area occupied by the $1s$ electrons. The $2s$ shell will thus be pushed outside the $1s$ one. Carrying on, the building principle works in a similar way. Electrons do gather in shells, characterized by a principal ($n = 1, 2, 3 \ldots$) and an orbital quantum number ($l = 0 \equiv s$, $l = 1 \equiv p$, $l = 2 \equiv d$, $l = 4 \equiv f \ldots$) where each l shell contains $2(2l+1)$ electrons. In light atoms (lighter than Ca (Z=20)) the sequence of successively occupied shells is $1s, 2s, 2p, 3s, 3p, 4s, 3d \ldots$. An example, for the electronic structures of Carbon (C), Fluorine (F), Neon (Ne), and Sodium (Na), is given in Figure 1.3. The single-electron energies have been obtained by density-functional methods as discussed in Chapter 3 which suffices for the purpose of the schematic discussion

here. The lowest level, the $1s$ shell, lies for all examples so deep that it does not fit into the given scale. We track here mainly the evolution of the $2s$, $2p$ and $3s$ shells in the vicinity of the rare gas Ne. The nuclear charge, and thus the electron number, increases from C to Na as $Z(\mathrm{C}) = 6$, $Z(\mathrm{F}) = 9$, $Z(\mathrm{Ne}) = 10$, and $Z(\mathrm{Na}) = 11$. The filling of the shells proceeds accordingly as indicated in the figure. Next to the element symbol we show also the spectroscopic notation for the shell filling. It is self-explanatory. The example also allows one to understand a widely used naming in molecular physics: one speaks of the highest occupied molecular orbital (HOMO) and lowest unoccupied molecular orbital (LUMO). The case is clearest for the rare gas Ne here. The HOMO is the $2p$ shell and the LUMO the $3s$. The energy difference, which often dominates excitation properties, is called the HOMO–LUMO gap.

The comparison of the various spectra in Figure 1.3 is enlightening. Indeed, although the atoms are quite close to each other in terms of size, they have very different properties. Compare, e.g., the cases of F and Na in which the HOMO in Na is much more loosely bound than in F. As we shall see below, this feature is at the origin of the different chemical reactivity of these two atoms. The energy difference between occupied and empty states also varies significantly from one element to the other. In all cases the empty states are only bound by a few eV at most, while the binding energy of the HOMO may vary between about 5 and 20 eV. Such differences in the spectra imply differences in the capability of electrons to be removed from an occupied to an empty state. In other words, not only binding properties of an assembly of atoms, but for example their response to a laser will significantly vary from one atom to the other. We shall see examples of such differences at various places below. Furthermore, we shall see that these four atoms exemplify the basic bonding types. And they have been used extensively in cluster studies (except maybe for the fact that the preferred rare gas for building clusters is Ar rather than Ne).

Going to heavier and heavier atoms the filling of electrons in shells becomes more and more involved. Nevertheless there exist the so called Hund's rules as reasonably robust guidelines for an estimate of the sequence of occupied levels, and of their degree of occupancy. The first rule states that electrons successively occupy the levels $1s$, $2s$, $2p$, $3s$, $3p$, $4s$, $3d$, $4p$, $5s$, $4d$, $5p$, $6s$ .... The rule is strictly correct as long as no d states are involved. As soon as d states enter the game, the actual electronic structures do not exactly match the filling of the shells monotonously but tend to oscillate between d and s while stepping up the elements. This first rule does not yet predict the electronic structure fully. An open question concerns degenerate levels. For example, in carbon, the occupied levels are indeed $1s$, $2s$, and $2p$ with the corresponding electronic structure $1s^2 2s^2 2p^2$. But the $2p$ state is $2\times$3-fold degenerate ($2p_x, 2p_y, 2p_z$ times spin) and the above electronic structure allows 2 out of 6, i.e. 15, equivalent choices. The second Hund's rule states that electrons occupy all degenerate subshells once *before* occupying any level twice. This nevertheless does not yet tell with which spin configuration this "democratic" filling is performed. This last open point is addressed by the third rule which states that the ground state configuration of an atom is the one with maximum net spin (namely aligned spins). There is a subtle detail to be observed, though, when applying the third rule. One has to count electron spins up to half filling and switch to hole spin for the upper half towards the next rare gas. All in all, Hund's rules, although with some exceptions, provide a useful guideline for predicting the electronic structure and the level filling in an atom. They are especially pertinent in small atoms.

The heavier the atom, the more shells are filled with electrons. However the simple systematic filling of a given sequence of levels is no more ensured in these heavy atoms and from one element to the next one may observe fluctuations in the filling. This is typically the case in the vicinity of the noble metals such as Ag, Au or Pt. For example, the last occupied shells of Ag (having $Z = 47$) are successively $4d$ with 10 electrons and $5s$ with one electron. On the basis of light atoms one would have expected a full s shell ($5s^2$) more bound than an open d shell ($4d^9$). This change is caused by small rearrangements of the mean field which influence the relative energy of $4d$ and $5s$ shells. The bigger surprise rather comes when looking at the whole sequence: Mo ($Z = 42$, $4d^5 5s$), Tc ($Z = 43$, $4d^5 5s^2$), Ru ($Z = 44$, $4d^7 5s$), Rh ($Z = 45$, $4d^8 5s$), Pd ($Z = 46$, $4d^{10}$), Ag ($Z = 47$, $4d^{10} 5s$). The $5s$ shell is alternatively filled or emptied depending on minimal energetic changes. Not surprisingly, in these cases where the two shells, $4d$ and $5s$, are energetically so close, the $4d$ and $5s$ electrons are likely to simultaneously play a role in low energy phenomena. The simplified discussion which we use here thus becomes insufficient for heavier elements. One needs to think of the spin-orbit splitting which can easily span the few eV energy differences discussed in the filling of transitional elements. The spin-orbit force is also crucial for the magnetic properties which also show their most dramatic consequences for transitional elements, particularly Fe, Ca, and Ni.

1.1.1.2 The atomic many-body problem

It is obvious from the above qualitative discussion that there is no trivial model to understand the details of the filling of electron shells. The problem is complex and of many-body nature. The atomic nucleus provides an attractive potential. The quantum mechanics of that is well known as it constitutes a central field problem for *one* electron. The difficulty comes from the electron–electron interactions for *several* electrons simultaneously. Qualitatively, and to some extent quantitatively, this many body nature of the problem manifests itself in terms of screening. In other words, one electron essentially feels the nuclear field screened by the electrons belonging to the more bound shells. But the balance is more delicate. First, as already mentioned, one has to account for the Pauli principle which repels outer electrons from the central part of the atom. This exclusion effect still preserves the sphericity of the problem. More delicate is the fact that electrons belonging to the same shell also repel each other via the Coulomb interaction. And such an effect has to be accounted for on a one to one basis. Stated so crudely, the problem might appear as awfully complicated. It is indeed, if one looks for spectroscopic details. Global features, however, are more forgiving. The key mechanism of simplification lies here in the presence of the external field provided by the nucleus. Indeed, in spite of the electron–electron corrections, this central attracting field somewhat shapes the gross structure of the electronic spectrum and basically sets a hierarchy in the way one accounts for electron–electron effects. To an acceptable approximation, the simple screening picture can thus be recast into a self consistent mean field approach in which each electron feels an average potential field created by the nucleus and the electron–electron interactions (including both intra and inter-shell interactions). This is the spirit of the so called "central field" approximation. Let us briefly explain what lies behind this concept.

We start from the many body electron Hamiltonian for an atom with N electrons (positions $\mathbf{r}_i$) bound to a nucleus of charge Z

$$H = \sum_i^N (-\frac{\hbar^2}{2m_e}\nabla_i^2 - \frac{Ze^2}{r_i}) + \sum_{i<j}^N \frac{e^2}{|\mathbf{r}_i - \mathbf{r}_j|} \tag{1.1}$$

where m_e is the electronic mass (note that we are using the Gaussian system of units, see Appendix A.1). The central field approximation of Hartree and Slater [Har27, Sla51] is based on an independent particle picture. One admits that electrons do move in an effective potential representing the nuclear attraction together with the repulsive interactions with the remaining $N-1$ other electrons. As discussed above, the major effects of these $N-1$ electrons is to screen the nuclear charge. Thus the inter-electron repulsive term contains a large spherically symmetric component which we shall write as $\sum_i U_{\rm H}(r_i)$. This means that we can approximate the effective potential field felt by one electron by a spherically symmetric potential

$$U_{\rm total}(r) = -Ze^2/r + U_{\rm H}(r) \quad . \tag{1.2}$$

The actual form of $U_{\rm H}(r)$ remains to be specified. The asymptotic behaviors can be easily fixed by requiring recovery of the nuclear field at short distance and of the net charge felt by the last electron at large distance, namely

$$U_{\rm total}(r) \underset{r \to 0}{\longrightarrow} \frac{-Ze^2}{r} \qquad , \qquad U_{\rm total}(r) \underset{r \to \infty}{\longrightarrow} \frac{-(Z-N+1)e^2}{r} \quad . \tag{1.3}$$

The determination of the effective potential at intermediate range is of course more involved as it requires one to account for all the electrons. Many methods have been developed to attack this problem. Let us cite the most famous Thomas-Fermi and Hartree-Fock methods, which both provide a well defined way to compute a central field, actually a mean-field potential common to all the electrons constituting the system (for a detailed discussion and references see Chapter 3). The central field approximation turns the initial three dimensional (3D) problem into an effective spherical 1D problem, which can fairly easily be solved with standard techniques of basic quantum mechanics. The N-electron wavefunction is factorized into N one-electron wavefunctions, which in turn can be factorized into a radial and an angular part $\varphi_{nlm}(\mathbf{r}) = R_{nl}(r)Y_{lm}(\theta,\phi)$ (with obvious notations). The resolution of the radial Schrödinger equation provides the $R_{nl}(r)$ and the corresponding principal ($n = 1, 2, 3\ldots$) and orbital ($l = 0, 1, 2\ldots$) quantum numbers. There is one subtle feedback loop in that treatment: the effective central field is composed from the Coulomb force of actual electron densities; these, in turn, depend on the central field. The problem is then resolved by iterating the solution with subsequent update of the central field until the feedback loop has converged. After all one disposes of the sequence of one-electron energies in levels $1s, 2s, 2p, 3s, 3p, 4s\ldots$, as already discussed above. Of course the details of the level filling may vary from one atom to the next, an effect which is related to the actual form of the central field $U_{\rm total}(r)$ and its self-consistent arrangement. Such mean field models are widely used in atomic physics and provide a sound starting basis for more elaborate approaches, taking better into account correlations between electrons. The density functional theory in which these correlations are

expressed in terms of the local electronic density (see Section 3.3.3) offers here a robust starting point for such investigations. A first example of applications of this method was given in Figure 1.3 showing the spectra of the four simple atoms C, F, Ne, and Na.

A comment is in order here concerning the meaning of single electron energies, and in particular its relation to experimental observables. When an atom is excited, for example by a laser, an electron may be promoted from one state of initial energy ε_1 to another of energy ε_2 (the latter being possibly unbound). Experimentally, one only can access the transition energy $\varepsilon_2 - \varepsilon_1$, for example through a photon. This provides the well known series of transition lines observed in various atoms. But one has to keep in mind that this electronic transition is a complex dynamical process which affects not only the "promoted" electron but the whole atom. Indeed, the energy levels of an atom with an empty electronic slot (called a *hole*, h) at level ε_1 and an (originally empty but now) occupied level ε_2 (called a *particle*, p) are different from the energy levels of the original atom ($0ph$). All the electrons in the excited ($1ph$) atom have to rearrange themselves to account for the electronic modification, and the energy levels do the same. This means in particular that, if the excited atom remains bound, the final energy of the "promoted" electron will not exactly be ε_2. As a consequence observing the transition energy gives a direct access neither to ε_1 nor to ε_2 of the original atom but includes corrections from a complex (specific) rearrangement process. An ideally instantaneous "promotion" of the electron (if possible) might leave the rest of the atom frozen and thus indeed give information on the actual energies of occupied levels in the original atom. In the other extreme case of an infinitely slow electronic excitation all other electrons do rearrange continuously and one will rather measure the energies of the final excited atom. The actual experimental situation usually lies in between these two extremes. We shall discuss similar examples in the case of clusters, see e.g. Sections 2.3.2 and 2.3.8. It is however to be noted that rearrangement effects are much larger in clusters than they are in atoms, because of possible ionic effects.

1.1.2 Molecules

1.1.2.1 The Mendeleev classification of elements

The successive filling of electronic shells provides the microscopic basis for the understanding of chemical properties of elements. Indeed, the early Mendeleev classification, although initially founded on mass rather than on electron number, was precisely trying to explain the regularity observed in the chemical reactivity of apparently different atoms. Since then we have learned that these chemical similarities reflect the behavior of the tiny fraction of least bound electrons in atoms, the so called valence electrons. And as long as valence electrons belong to shells with the same angular momenta ($s, p, d \ldots$ shells) the corresponding atoms behave similarly at the chemical level. This is, after all, not so surprising. The value of the angular momentum of the shell fixes the shape of the electronic wavefunctions and hence the capability of a given electron of a given atom to interact, and possibly bind, with electrons of another atom. The degree of filling also fixes the capability of an atom to accept or to release valence electrons. The atoms with completed shells (shell closure) are especially stable. The so called rare gases (He ($Z = 2$), Ne ($Z = 10$), Ar ($Z = 18$), Kr ($Z = 36$), Xe ($Z = 54$), and Rn ($Z = 86$)) form the family of the most stable atoms. They have the highest values of ionization potential. This explains why these species are particularly inert from the chemical

point of view. In the "vicinity" of these rare gases lie two categories of atoms either with one electron more or one electron less than the corresponding rare gas. In turn, these two families of atoms are extremely active from the chemical point of view because the atoms belonging to these families have a strong tendency either to grab or to release an electron, in order to attain an electronic configuration similar to that of the neighbor rare gas. The alkaline atoms (Li ($Z = 3$), Na ($Z = 11$), K ($Z = 19$), Rb ($Z = 37$), Cs ($Z = 55$), Fr ($Z = 87$)) have one valence electron belonging to a s shell as compared to the neighbor rare gas. This s electron is weakly bound, which implies a small ionization potential. Correlatively, it has a strong tendency to leave its parent atom, as we shall see below. On the contrary, the halogen atoms (F ($Z = 9$), Cl ($Z = 17$), Br ($Z = 35$), I ($Z = 53$), At ($Z = 85$)) exhibit a valence p shell missing one electron for closure. They thus have a strong tendency to find this electron in their surrounding. Obviously alkaline and halogen atoms are likely to "complement" each other. An alkaline atom will tend to "give" its peripheral s electron to a halogen atom to complete its p shell. This exchange of electrons forms the basis of the most robust chemical bond, the ionic bond in which electron exchange ensures a robust electrostatic binding between two charged species, a positively charged alkaline and a negatively charged halogen. We shall come back to this below. But before exploring more systematically binding possibilities between atoms, one has first to come back to the Mendeleev classification for a few more remarks. Up to now we have discussed only 3 columns of atoms (rare gas, alkalines, halogens) while the Mendeleev classification contains up to 18 columns. In fact, halogens and alkalines, as "ends" of each row do represent the extremes cases of tendencies which develop along each row of the classification. Starting from an alkaline atom, successively adding electrons (namely going in the direction of the next heavier halogen) will progressively attenuate the tendency of the atom to release electrons and increase its tendency to grab them. There is thus a continuous path between electron donors and electron acceptors. In the middle of the path lie atoms with an "equal" tendency to grasp or to release electrons. The typical representatives of this class are carbon (C, $Z = 6$) silicon (Si, $Z = 14$) and germanium (Ge, $Z = 32$). We shall see that they tend to bind between each other in a specific way giving rise to a very rich palette of molecular structures, particularly for carbon.

1.1.2.2 A pedestrian view of bonding

The first step along the path from atoms to molecules (and to clusters) is represented by dimer molecules and we shall here focus on this simple case. As already mentioned, depending on their electronic structures two atoms may, or may not, bind together, with different type and strength of binding. Chemical binding is by nature a low energy phenomenon, involving at most a few eV energy. For this reason only valence electrons significantly play a role, and the Mendeleev classification thus provides a gross map of which atom may possibly bind with which other and how. Of course, binding between two atoms is a matter of electrons and energy. The key question is thus whether the valence electron(s) of a given atom may find it energetically interesting to "leave" their parent atom to "bind" to another atom, or whether there are "intermediate" solutions for these electrons, like partial attachment to both atoms. According to such a simple picture, one may envision four classes of binding reflecting the possibility of sharing the set of valence electrons between the two partner atoms, as illustrated in Figure 1.4. As in any scheme, these bonding types are idealized extremes. Real molecules are usually dominated by one of these bondings with admixtures of the complementing types.

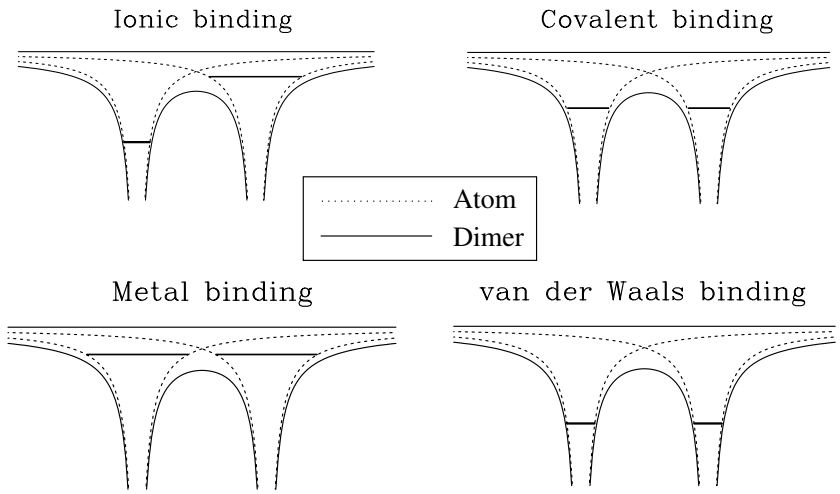

Figure 1.4: Schematic view of potential and valence levels in dimers with the four basic types of binding as indicated. The molecular potential is drawn with solid lines and the atomic one with dashed lines. The valence levels are indicated by horizontal straight lines.

The first possibility is ionic binding. One loosely bound electron is transferred from its parent atom to a host atom in which it finds an empty slot on a more deeply bound level. The electronic energy level in the parent atom is less bound than the host level and the transfer becomes easier if the possible potential barrier between the two atoms is smaller. In other words, the smaller the ionization potential of the parent atom, the easier the transfer. Because the difference in the electronic levels of the donor and the acceptor is large the exchange is indeed effective. The electron localizes predominantly on the host atom. The exchange of the electron thus charges positively the donor atom and negatively the acceptor atom. This gives rise to what is known as an ionic bond, in which a positive charge is concentrated on one atom and a negative charge on the other atom, making the system almost a +/- ionic dimer. Typical examples of ionic binding are realized between alkaline (electron donor) and halogen (electron acceptor) atoms, as explained above. Everyday kitchen salt (NaCl) crystals are bound with such a mechanism. The large energy gain associated with the electron exchange explains the robustness of the ionic bond.

When the energy difference between the valence shells of the two atoms is not so large, electron transfer becomes unfavorable and electrons tend to remain close to their parent atoms. This does not exclude binding. But then binding stems from charge sharing rather than charge transfer. The valence electrons tend to form a common electronic cloud establishing the binding of the two atoms together. The properties of this common valence cloud again depend on the nature of the partner atoms and may give rise to two different types of binding. The binding energy of the atomic valence electrons determines the behavior. If the valence electrons are weakly bound the electronic wavefunctions can easily spread outside the parent atoms. As soon as the proximity of the partner atoms has sufficiently decreased the barrier between them (see Figure 1.4), the electronic wavefunctions become delocalized all around the two atoms

and one then speaks of a metallic bond (as a precursor of the behavior of such systems in the bulk, discussed below). Alkalines are the typical elements which establish metallic bonds between each other. They are called simple metals because of the well separated valence electron (see Na in Figure 1.3). We shall often consider the generic example of Na_n clusters as typical simple metallic systems. Metallic binding is also observed in more complicated metals such as, e.g., Cu, Ag, Au, or Pt. The valence binding mechanism in these systems is qualitatively similar to the simple case of alkalines, but there is then a d shell energetically close to the valence s shell (see the example of Cu in Figure 3.2). This causes strong polarization effects with impact on binding and other dynamical properties (see e.g. the discussion of optical response in Section 4.3.4.1).

The metallic binding does not exhaust all possibilities of sharing a common valence cloud. If the electrons are initially more strongly bound to their parent atom, electron delocalization cannot fully develop and electrons gather in the region of smallest potential energy, between the two partner atoms. One then speaks of a covalent bond. The typical covalent bond is realized between atoms like C or Si in which atomic valence electrons are fairly well bound (see also Figure 1.3). However, one has to keep in mind that covalent and metallic bonds are idealized situations. There is a smooth transition between these extremes. It is usually hard to disentangle these two types in small molecules. The distinction becomes better defined in bulk material where interstitial density and conductivity add useful criteria [AM76].

When valence electrons are too deeply bound in the atom, neither charge transfer nor charge sharing are possible between the two atoms. Because the HOMO electrons are too deeply bound, the electrons cannot escape the attraction of their parent atom. One may then wonder how bonding is possible at all. Although electrons remain localized around their parent atom, the electronic cloud of each atom is influenced by the partner atom. This virtual polarization of the electronic clouds results in mutual dipole-dipole interactions between the two atoms, which establishes a binding of the system. As is obvious the resulting bond is much weaker than the previous ionic, metallic or covalent bonds. And yet, it suffices for the binding of rare gas molecules up to possibly large compounds, as we shall see below. This type of loose binding is known as van der Waals (or molecular) binding, in reference to the interactions between two neutral atoms or molecules. The typical cases of van der Waals bonding thus concern rare gas atoms mostly. It should be noted that the details of the binding mechanism are somewhat involved. The polarization of the electronic cloud has to be understood as a dynamical correlation effect, with constantly fluctuating dipoles, rather than as a mere static polarization. To properly account for this effect requires a quantum mechanical treatment which we shall not discuss here.

All in all, simple energetic considerations for the HOMO, as exemplified in Figure 1.3, allow one to identify four major types of bonding between atoms, as schematically represented in Figure 1.4. These energetic aspects reflect themselves in the degree of localization of the electrons binding the two atoms: the more bound the electrons, the more localized their wavefunctions. Of course, just like the behavior of atoms as electron donors or acceptors, there is no clear separation between the various binding mechanisms, but rather a continuous path between them (see Figure 1.8 for an example in the bulk). Still, the four classes identified above can be seen as robust guidelines for understanding the binding of most molecular systems. Finally, it should be noted that one sometimes introduces a few other classes of binding. The term “molecular binding” for example refers to the binding between molecules, while the term

"van der Waals" usually concerns atoms, although in both cases the basic binding mechanism is the same. Similarly one sometimes speaks of "hydrogen bonding" to label covalent binding involving hydrogen atoms. Because its particularly large ionization potential, hydrogen usually establishes especially robust bonds (as compared to standard covalent bonds) with other species, hence the specific label. Again, such fine distinctions do not basically alter our global classification scheme. We shall thus ignore such details in the following.

1.1.2.3 Deeper into microscopic mechanisms

Before proceeding to the bulk (in Section 1.1.3) and to clusters (in Section 1.2) we would like to discuss in some more detail the binding mechanism for simple dimers, in order to exhibit the dominant mechanisms in a semi-quantitative fashion. We keep the discussion at a minimal level of formalism. More detailed elaborations of that sort can be found in many standard textbooks on molecular physics or chemistry (see Appendix A.4).

We consider the case of a dimer formed from two atoms A and B, each having *one* s valence electron (as is the case for H or Na). The atoms are placed at a distance R from each other. We denote by φ_A and φ_B the respective atomic single-electron wavefunctions following the Schrödinger equations

$$-\frac{\hbar^2}{2m}\Delta\varphi_X + V_X\varphi_X = \varepsilon_X\varphi_X \quad , \quad X \in \{A, B\} \quad , \tag{1.4}$$

where V_X labels the potential felt by the valence electron in atom X and ε_X is the corresponding eigenvalue of energy. In order to simplify the problem further, we restrict ourselves to the case of an ionized dimer, in which only *one* active electron is left (as in H_2^+ or Na_2^+). The goal is then to solve the Schrödinger equation for the dimer electron

$$-\frac{\hbar^2}{2m}\Delta\varphi_{AB} + V_{AB}\varphi_{AB} = \varepsilon_{AB}\varphi_{AB} \quad , \tag{1.5}$$

where ε_{AB} labels the energy of the electron level binding the dimer. The total potential V_{AB} is, in principle, a self consistent quantity as it depends on the wavefunction φ_{AB} itself, because the formation of the bond induces an electronic rearrangement and thus a modification of the net atomic fields. For the sake of simplicity and because these rearrangement effects can be assumed reasonably weak, at least for an exploratory approach, we approximate V_{AB} by

$$V_{AB} \simeq V_A + V_B + \frac{e^2}{R} \quad . \tag{1.6}$$

For the solution we assume that we can represent the molecular electronic wave function φ_{AB} in terms of the given atomic wave functions. This means that we make the ansatz of Linear Combination of Atomic Orbitals (LCAO)

$$\varphi_{AB} = c_A\varphi_A + c_B\varphi_B \quad . \tag{1.7}$$

It remains to determine the expansion coefficients c_A and c_B.

Variation of the total energy with respect to these coefficients yields in a straightforward manner the secular equation

$$\begin{pmatrix} \tilde{\varepsilon}_A + \frac{e^2}{R} & (\bar{\varepsilon} + \frac{e^2}{R})S + h \\ (\bar{\varepsilon} + \frac{e^2}{R})S + h & \tilde{\varepsilon}_B + \frac{e^2}{R} \end{pmatrix} \begin{pmatrix} c_A \\ c_B \end{pmatrix} = \varepsilon_{AB} \begin{pmatrix} 1 & S \\ S & 1 \end{pmatrix} \begin{pmatrix} c_A \\ c_B \end{pmatrix} \quad (1.8)$$

where

$$S = \int d\mathbf{r} \varphi_A^* \varphi_B \quad , \quad h = \int d\mathbf{r} \varphi_A^* \bar{V} \varphi_B \quad ,$$
$$\tilde{\varepsilon}_A = \varepsilon_A + \int d\mathbf{r} \varphi_A^* V_B \varphi_A \quad , \quad \tilde{\varepsilon}_B = \varepsilon_B + \int d\mathbf{r} \varphi_B^* V_A \varphi_B \quad ,$$
$$\bar{\varepsilon} = \frac{\tilde{\varepsilon}_A + \tilde{\varepsilon}_B}{2} \quad , \quad \bar{V} = \frac{V_A + V_B}{2} \quad .$$

The key quantities for the mixing are the overlap (S) and bond (h) integrals. They provide measures of how much the two electronic wavefunctions "communicate", either "directly" (overlap integral) or via the interaction (bond integral). In the limit of a sufficiently small overlap integral S the two solutions $\varepsilon_{AB}^{+,-}$ of the secular equation Eq. (1.8) take the simple forms ($\Delta\varepsilon = \varepsilon_A - \varepsilon_B$)

$$\varepsilon_{AB}^{\pm} = \bar{\varepsilon} + |h|S \mp \sqrt{h^2 + \Delta\varepsilon^2/4} \quad (1.9)$$

where the most bound level ε_{AB}^{+} is known as the bonding state while the least bound one ε_{AB}^{-} is the antibonding state. Both the bond and the overlap integrals enter the expressions of $\varepsilon_{AB}^{\pm}$. Because by construction the bond integral is less than 1, the bonding state is always more bound than the most bound atomic level $\varepsilon_{AB} \leq \min(\varepsilon_A, \varepsilon_B)$ (note that the cross-over elements are negative, e.g. $\int d\mathbf{r} \varphi_A^* V_B \varphi_A < 0$), which is what establishes binding. The net gain of binding then depends on S and h, which points out the importance of the capability of electrons to explore the partner atom (S and h). Note finally that the energy separation between bonding and antibonding states increases with the bond integral. These behaviors are illustrated for the case of homonuclear dimers in the schematic Figure 1.5. Note that here $\varepsilon_A = \varepsilon_B$ and thus $\Delta\varepsilon = 0$. The lower part shows how the matrix elements S and $|h|$ decrease quickly as a function of molecular distance R. Similarly behaves the convergence $\varepsilon_{AB}^{\pm} \longrightarrow \bar{\varepsilon} = \varepsilon_A = \varepsilon_B$ for large R.

The energetic information provided by Eq. (1.9) can be nicely complemented by looking at the spatial extension of the electronic cloud. The interesting quantity is here the electronic density $\rho_{AB}^{+}(\mathbf{r}) = |\varphi_{AB}^{+}(\mathbf{r})|^2$ of the bonding state. It reads

$$\rho_{AB}^{+}(\mathbf{r}) = (1+\alpha_i)\rho_A(\mathbf{r}) + (1-\alpha_i)\rho_B(\mathbf{r}) + \alpha_c \rho_{\rm bond}(\mathbf{r}) \quad , \quad (1.10a)$$
$$\rho_{\rm bond} = 2\varphi_A^* \varphi_B - S(\rho_A + \rho_B) \quad , \quad (1.10b)$$
$$\rho_X = \varphi_X^* \varphi_X \quad \text{for} \quad X \in \{A, B\} \quad , \quad (1.10c)$$
$$\alpha_c = \left[1 + \frac{\Delta\varepsilon}{2|h|}\right]^{-1/2} \quad , \quad \alpha_i = \frac{\Delta\varepsilon}{2|h|}\alpha_c \quad . \quad (1.10d)$$

The relations simplify in the homonuclear case, where $\Delta\varepsilon = 0$, to $\alpha_c = 1$, $\alpha_i = 0$ and finally to $\rho_{AB}^{-} = \rho_A + \rho_B + \rho_{\rm bond}$. It shows that the bond density makes all the difference.

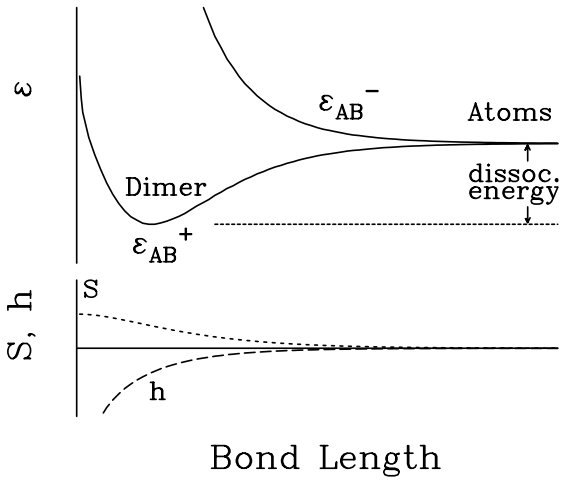

Figure 1.5: Schematic plot of the overlap (S) and bond (h) integrals (bottom part) and of the energies of the bonding (ε^+_{AB}) and antibonding (ε^-_{AB}) levels as a function of distance R between the two atoms. Scales are arbitrary, but note that the overlap integral tends towards 1, at short R. Asymptotically (large R) both S and h integrals vanish and $\varepsilon^\pm_{AB} \to \bar{\varepsilon}$, namely the dimer becomes a collection of two independent atoms. The dip in (ε^+_{AB}) at finite distance corresponds to the bond length, namely the equilibrium distance d_b between the two bound atoms forming a dimer. The difference between $\varepsilon^\pm_{AB}(d_\mathrm{b})$ and ε_A (or ε_B) represents the dissociation energy of the dimer.

Let us briefly discuss the case of a heteronuclear system ($A \neq B$) which is already prepared in the above equations. The difference $\Delta\varepsilon \simeq \varepsilon_A - \varepsilon_B$ shows up at the level of the bonding and antibonding energies. Note that the energy of the bonding state, and thus the nature of binding also depend on the energy difference between the two original atomic orbitals. It also sensitively enters the total electronic density $\rho_{AB}(\mathbf{r})$ given in Eq. (1.10). The now non-trivial parameter α_i provides a measure of the ionic charge renormalization, hence of the amount of electron density transferred from one atom to the other. Obviously the most covalent bond corresponds to $\alpha_i = 0$, as is the case in a homonuclear system. Otherwise, if $\alpha_i > 0$ ($\varepsilon_A \leq \varepsilon_B$), the electron density gathers around A as in a more or less ionic bond. All in all, the two parameters α_i, α_c thus provide a measure of the degree of ionicity of the bond, allowing one to span in a continuous way the various situations between pure covalent ($\alpha_i = 0$, $\alpha_c = 1$) and pure ionic ($\alpha_i = 1$, $\alpha_c = 0$) binding.

1.1.2.4 More realistic examples

For sake of simplicity, we have restricted our discussion, up to now, to the case of ionized dimers, with only one active valence electron. Passing to neutral dimers is qualitatively easy to grasp, but computationally more involved. As soon as two electrons, one from each atom, bind together, one has to take into account the Coulomb repulsion between the two electrons. It affects both the energies $\varepsilon^\pm_{AB}$ and the repartition of the electronic density $\rho_{AB}(\mathbf{r})$. Nonetheless, the above discussions remain qualitatively valid, in particular concerning the roles of the parameters governing the basic properties of the bond (bond and overlap integrals, energy difference $\Delta\varepsilon$). To obtain quantitative results in practice, an explicit and detailed calculation of electronic structure has to be performed, starting from a microscopic description of each atom, usually including more than only valence electrons. And it will turn out that the details of electronic spectra (both occupied and empty states) are actually to be accounted for. We will address these theoretical methods in Chapter 3.

type	v. d. Waals	metallic	covalent	ionic
example	Ar_2	Na_2	C_2	NaF
D [eV]	0.010	0.74	6.2	5.0
d_b [a_0]	7.1	5.8	2.3	3.5

Table 1.1: Dissociation energy D and bond length d_b for selected diatomic molecules, each one representing one bond type as indicated. Data from [AM76, Bei95, Kra96, GLC+01].

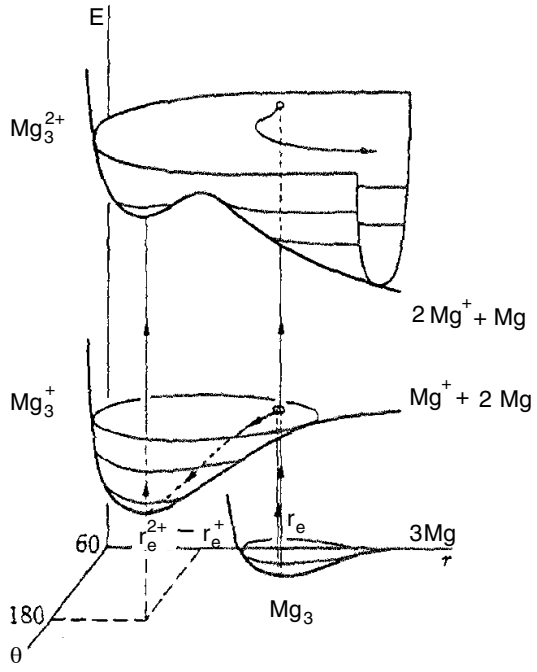

Figure 1.6: Born-Oppenheimer surface for the dissociation of Mg_3 possibly with electron emission. The considered dissociation channels are here $Mg_3 \longrightarrow Mg^+ + 2Mg + e^-$ and $Mg_3 \longrightarrow 2Mg^+ + Mg + 2e^-$. The potential energy surfaces of Mg_3, Mg_3^+ and Mg_3^{2+} are thus drawn together with the corresponding dissociation paths. Note the various dissociation paths for the doubly charged species as a function of ionization mechanism (see text for details). After [DDM86].

Here we continue the discussion with a few realistic data for simple molecules. The energy curves look qualitatively all very similar to the schematic view in Figure 1.5. What changes is the depth and position of the potential well. It can be quantified in terms of the dissociation energy D as the difference between the asymptotic energy and the bonding minimum (see Figure 1.5) and of the bond distance d_b which is the distance where the minimum resides. Table 1.1 gives a few examples for the four typical bond types discussed above. The van der Waals binding is the weakest by far. Covalent and ionic binding are the strongest and the metallic example is slightly weaker than these.

A more complex case is demonstrated in Figure 1.6. It is the Born-Oppenheimer molecular energy surface (Appendix C.1) for the dissociation of Mg_3. Also are represented the potential energy surfaces for Mg_3^+ and Mg_3^{2+}.

The surfaces are plotted as a function of a typical distance and angle. The Mg_3 cluster structure can obviously be represented by two such parameters and the same holds for both Mg_3^+ and Mg_3^{2+}. One ought to realize, though, that the example of this figure corresponds to

a particularly simple case, because of the small size of the system. A complex molecule (or cluster) has many ionic degrees of freedom. The molecular energies thus correspond to huge multi-dimensional Born-Oppenheimer surfaces from which one can inspect at most well taken cuts. Such large systems are treated in practice by more direct dynamical methods as will be outlined in Chapter 3.

Several dissociation channels are sketched in Figure 1.6, depending on the degree of ionization (singly or doubly charged Mg_3). As can be seen from the figure the corresponding potential energy surfaces do differ in shape. For example one sees that the more charged the cluster, the more compact the ground state configuration, corresponding to the minimum of the potential well. The figure also demonstrates the various possible dissociation paths as a function of the excitation process. When the cluster is only singly charged it still corresponds, not surprisingly, to a well stable species. When it is doubly charged the picture becomes more involved. Indeed, if electron removal is sequential, the system, having lost one electron, may have time to relax towards the corresponding equilibrium Mg_3^+ state, before a second ionization promotes it, again, towards an equilibrium (although very weakly bound, and thus probably metastable) state, this time for Mg_3^{2+}. On the contrary, in the case of a simultaneous double ionization the system is immediately promoted towards an unstable configuration which directly dissociates. We find here an illustration, in the case of a small cluster, of the importance of the details of the dynamics in the ionization process. We shall come back to this question at many places (see for example Sections 2.3.2 and 2.3.8).

1.1.3 The point of view of solid state physics

Complementing the discussion on atom and molecule, we now turn to bulk matter. Bulk might have two different meanings in the case of clusters. Clusters are often in a liquid state, because of their high formation temperature (Section 2.1.3.1). When extrapolating, bulk then refers to a macroscopic liquid. But the ground state (low temperature state) of a cluster stays in a frozen geometry, and bulk then refers to an infinite solid, more precisely a crystal. In the following discussion we shall only consider this zero temperature situation and bulk will thus mean a piece of solid material.

From the viewing angle of solid state physics, a key parameter of classification is the conductivity of a given piece of material. One will thus separate solids into two classes: conductors and insulators. The different bonding types will be associated to these two classes. We shall first, as in the case of atoms/molecules, consider the problem at a qualitative level, before addressing the question from a more formal point of view.

1.1.3.1 Bond types in solids

The four classes of binding (metal, covalent, molecular and ionic) in the bulk are illustrated in Figure 1.7 for a set of typical examples. We will discuss them now step by step.

Metals constitute the class of conducting solids. In that case the valence electrons of each atom are fully delocalized, so that they form a nearly free uniform gas of electrons. Each electron thus loses any direct contact with the atom it was originally bound to. The typical (and simplest) examples of metallic bonding are again found in alkalines such as Na or K. The case of alkali metals is in some sense too clean. Indeed, one can find additional aspects

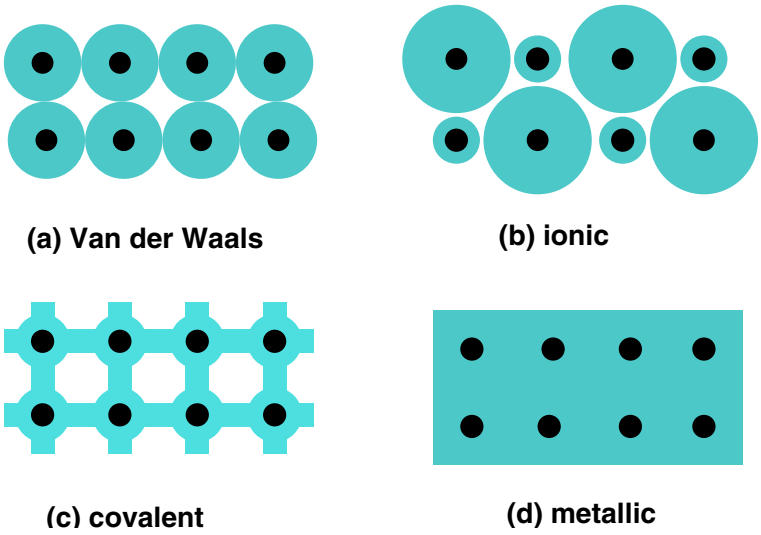

Figure 1.7: Schematic representation of electronic charge distributions in examples of solids. The small (filled) circles represent the ionic cores, with the corresponding "effective" charges seen by the electrons constituting the binding. The shaded areas represent regions in which one finds an appreciable amount of the electron density. Note that the electronic density is not uniform. The four cases correspond to the basic four types of binding: a) van-der-Waals (molecular) binding in an Ar crystal, b) ionic binding in KCl, c) covalent binding in C and d) metallic binding in K. After [AM76].

of van der Waals or covalent bonding in many metals, particularly in noble metals where loosely bound d electrons participate in the bonding. A typical example is Ag, in which the least bound electron belongs to a $5s$ shell, while the loosely bound $4d$ orbitals are strongly distorted by the presence of neighbor atoms. In such a case the separation between valence and core electrons is much less clear than in alkalines. And yet, such materials do also exhibit a clearly metallic behavior.

Materials with a poor conductivity belong to the category of insulators. But contrarily to the class of metals, bonding in insulators covers different forms, essentially reflecting the degree of localization of electrons around their parent atom. Let us successively consider these various bindings as a function of the degree of localization of electrons, while keeping in mind that the largest degree of delocalization is attained in metals.

In covalent crystals, one faces a set of semi-localized electrons, which gather along the lines joining atoms together. The typical example of such a binding is the case of diamond. Just as in simple molecules, we find a covalent nature of binding in carbon based materials.

The last two classes of insulators leave electrons fully localized on atomic sites. In van-der-Waals crystals such as solid noble gas (e.g., Ne, Ar, Kr, or Xe), very few electrons gather between the sites. Electrons basically remain bound to the original atom they were attached to. Just as in simple molecules, polarization effects are responsible for the binding of the system. The last class of compounds are ionic crystals which associate metallic (electron donor) and non-metallic (electron acceptor) atoms in a regular manner, so that ionic bonds

(see Section 1.1.2.2) can be reconstituted. In that case electrons are highly localized on atomic sites, once they have been transferred from the metal to the non-metal atoms. The typical example of such systems are alkaline halogen compounds such as NaCl, NaF, or LiF.

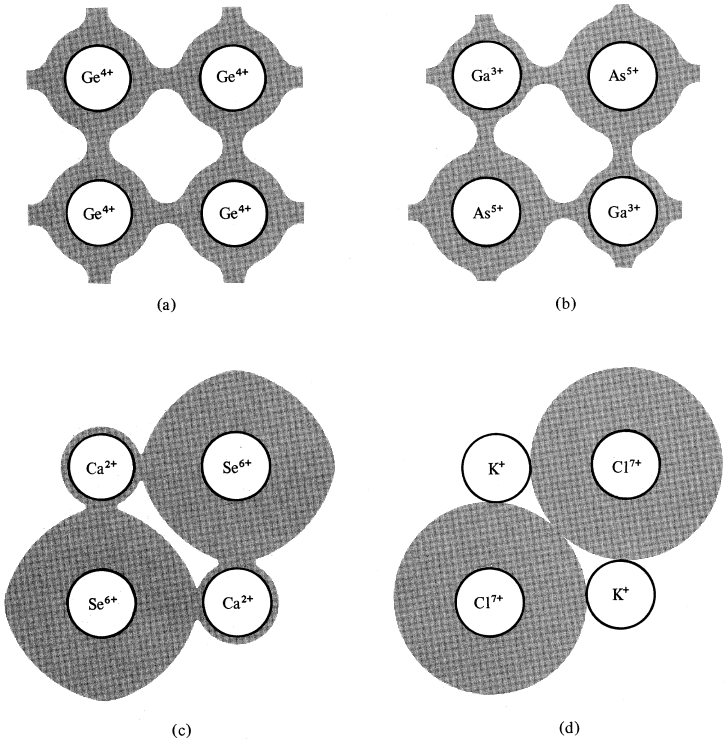

Figure 1.8: Schematic representation of the path between a perfectly covalent and a perfectly ionic crystal. a) Perfectly covalent Ge crystal: in this case 4 electrons are identically distributed about the Ge^{4+} cores; the electronic density is large along the interstitial directions; b) Covalent GaAs crystal: again density along the interstitial directions, but the electrons gather more around As^{5+} than around Ga^{3+}, which gives a slightly ionic character to the system. c) Even more ionic CaSe crystal: the trend of GaAs is even enhanced in that the Ca^{2+} cores are almost denuded of electrons, to the benefit of the Se^{6+} cores; still, the crystal keeps a slight covalent character. d) Perfectly covalent ionic KCl crystal: electrons have been fully stripped from the K and transferred to the Cl^{7+} cores. The electronic structures of the atoms considered here are: Germanium (Ge, (Ar)$3d^{10}4S^2 4p^2$), Gallium (Ga, (Ar)$3d^{10}4S^2 4p$), Arsenic (As, (Ar)$3d^{10}4S^2 4p^3$), Selenium (Se, (Ar)$3d^{10}4S^2 4p^4$), Calcium (Ca, (Ar)$4s^2$), Chlorine (Cl, (Ne)$3s^2 3p^5$) and Potassium (K, (Ar)$4s^2$). From [AM76].

It is clear from the above brief discussion that the solid state physics classification of bonding, not surprisingly, matches the classification of molecular physics. The analogies go even further. It was already discussed for molecules in Section 1.1.2 that the four types of bonding are idealizations and that reality often resides in between. Figure 1.8 complements that for crystals showing the path from covalent to ionic binding. Starting from the covalent Germanium crystal one observes, by associating successively atoms on both (complementing)

sides of Ge, a continuous transition towards the ionic KCl crystal. As we shall see below, clusters provide here an even more interesting option. They allow one to span a continuous path from atom to bulk. And one finds situations where the nature of bonding changes with system size.

1.1.3.2 Band theory in solids

A general theory of bonding in solids can be found in many specialized textbooks [AM76, Pet95]. We give here a brief summary of level structure in solids, and discuss how such a level structure is related to the nature of bonding. We start with a simple model crystal in 1D. The ionic lattice introduces an attractive potential $U(x)$ which alters the otherwise free motion of electrons and turns out to be responsible for the level structure. Taking a mesh size a, lattice periodicity implies a specific form for electron orbitals

$$U(x+na) = U(x) \quad \Longrightarrow \quad \varphi_k(x+na) = \exp(ikna)\varphi_k(x) \tag{1.11}$$

where n means any integer and k is the so-called lattice momentum. As is clear from this form of the wavefunction (Bloch ansatz), it is sufficient to consider values of k in the first Brillouin zone defined by $-\pi/a \leq k \leq \pi/a$. Other values only repeat phase factors $\exp(ikna)$ from the first zone.

The problem thus amounts to solving the Schrödinger equation for φ_k in an elementary cell $0 \leq x \leq a$ with the above defined periodic boundary conditions at $x = 0$ and $x = a$ (Bloch condition). For the sake of simplicity we assume that $U(x)$ is furthermore a square well potential of depth U_0 and width $a - b$, so that b also represents the barrier width between two neighboring wells, i.e.

$$U(x) = \begin{cases} -U_0 & \text{for } \left|\xi - \frac{a}{2}\right| \leq \frac{a-b}{2} \\ 0 & \text{for } \left|\xi - \frac{a}{2}\right| > \frac{a-b}{2} \end{cases} \quad , \quad \xi = \mod(x, a) \quad . \tag{1.12}$$

Inside the well, as is well known, the wavefunction takes an oscillatory form $\varphi_k(x) = A\exp(iKx) + B\exp(-iKx)$ where K is directly associated to the level energy E as $K = \sqrt{2mE/\hbar^2}$. Outside the well (or inside the barrier) the wavefunction takes an exponential form $\varphi_k(x) = A\exp(\kappa x) + B\exp(-\kappa x)$ with ($\kappa = \sqrt{2m(U_0 - E)/\hbar^2}$). The coefficients A, B, C, D are found by matching φ_k and $d\varphi_k/dx$ at boundaries $x = b$ and $x = a$ and imposing the Bloch periodic condition Eq. (1.11) on φ_k. This provides an implicit equation linking K, κ, k, b and a. For a qualitative discussion, we consider here the simple case of vanishingly narrow potential barrier $b \to 0$ and increasing barrier height $U_0 \to \infty$ (within imposing constant $U_0 b$). The implicit equation then reduces to the simple form

$$\cos Ka + \mu \frac{\sin Ka}{Ka} = \cos ka \qquad \text{with} \qquad \mu = \frac{ma}{\hbar^2} U_0 b \tag{1.13}$$

The above equation links the electron energy $E = \hbar^2 K^2/2m$ to the so called Bloch vector k. Bloch-like solutions φ_k therefore exist only for values of K, and hence E, which are solutions of Eq. (1.13) for a given k. Whatever k may be, the r.h.s. of Eq. (1.13) is bound by ± 1. The allowed values of K, and hence of electronic energies E, thus obey the constraint

$$|\cos Ka + \mu \frac{\sin Ka}{Ka}| \leq 1 \quad . \tag{1.14}$$

Except for the trivial case $\mu = 0$ which corresponds to the exact free electron gas (no ions, no potential), condition Eq. (1.14) provides the so called band structure of the electronic level scheme. Only certain bands of values for K (and E) are possible. The width of the bands depends on the effective strength μ.

Table 1.2: Lowest three bands (= allowed intervals) of K and E values in the simple 1D model for two values of μ. The low $\mu = 3$ (upper part) provides good conditions for a conductor. The large $\mu = 40$ (lower part) is an example for an insulator. The Ka are dimensionless. The translation into energies E used $a = 6\,\mathrm{a_0}$ for $\mu = 3$ and $a = 8\,\mathrm{a_0}$ for $\mu = 40$. The width was in both cases $b = a/2$.

	$\mu = 3 \longleftrightarrow$ conductor		
Ka	[2.03,3.13]	[4.38,6.28]	[7.13,9.38]
E [eV]	[1.56,3.71]	[7.27,14.96]	[19.30,33.40]
	$\mu = 40 \longleftrightarrow$ insulator		
Ka	[3.03,3.13]	[6.03,6.28]	[9.03,9.38]
E [eV]	[1.94,2.87]	[7.71,8.37]	[17.31,18.68]

Two typical examples, for a small one and a large value of μ, are given in Table 1.2. To translate the bands and gaps into energies, we have specified the lattice parameter a in each case.

A graphical view of the potentials, lattices, and bands for these cases is given in Figure 1.9. There appear forbidden energy ranges which correspond to gaps between the allowed energy bands. A gap structure, as exemplified in the above simple model, is a generic feature of level structure in solids. The details of band structures and gap sizes turn out to vary with the type of bonding in the considered sample. It can be discussed qualitatively within this simple model by a mere variation of the key strength parameter μ. The free electron gas limit is recovered for $\mu = 0$, in which case no gap appears and the electronic energy is of purely kinetic nature and can take any value. As soon as an interaction is introduced in the problem, forbidden energy regions appear, which means that, in spite of the fact that the system is infinite and the k index continuous in the first Brillouin zone, only bands of well defined energies are accessible and gaps reside in between.

Small values of μ correspond to the case of a nearly free electron gas and represent metallic systems. In that case, the energy gaps are small. And the valence band, namely the band with the HOMO is only partially occupied, see left part of Figure 1.9. In a metal, the Fermi energy ε_F lies in the middle of an allowed band. Any vanishingly small excitation of the electrons in this band thus allows them to be easily promoted from below the Fermi energy to one of the closely lying empty states. This is the reason why electrons can so easily move in a metal with virtually no energy consumption. This also explains the electric conductivity and the metallic character of such a system.

Larger values of μ correspond to systems in which the electrons remain more localized (large value of the potential depth or the barrier width) and can thus exhibit successively covalent and ionic bonding (see also Figure 1.8). The behavior is schematically illustrated

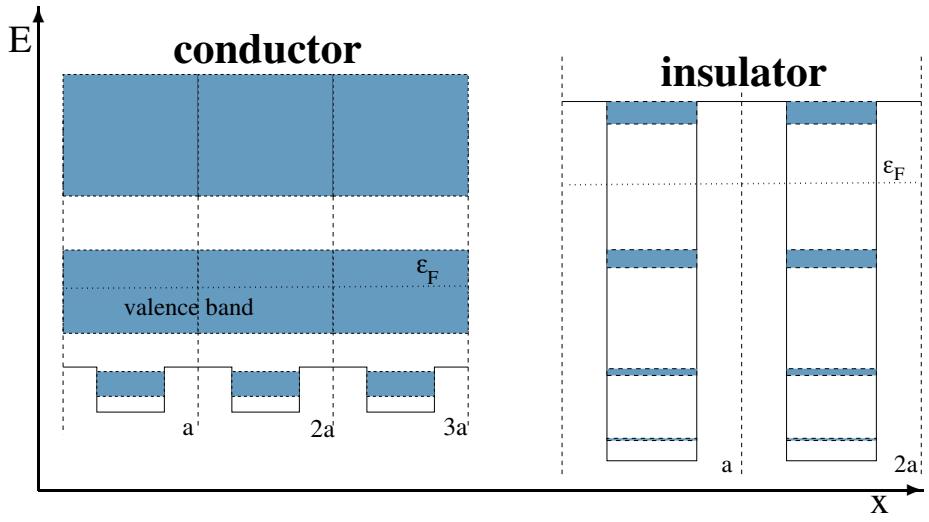

Figure 1.9: Schematic illustration of the band structure in a metal (left) and an insulator (right) according to the simple model discussed in the text (1D crystal with square potential wells). The allowed bands correspond to the shaded areas. Occupied levels are below the Fermi energy ε_F. Note that ε_F lies in the middle of an allowed band in the case of a metal, while it falls into a gap between two bands for an insulator.

in the right part of Figure 1.9 for a typical insulator (as obtained from the above schematic model). The Fermi energy ε_F now resides within a band gap. Promoting electrons from the highest occupied to the lowest unoccupied band now requires a sizable amount of energy. Conductivity in such systems is thus quite small, which explains the insulating character of the material.

Finally, the simple schematic model allows one to recover the case of molecular bonding in the limit of $\mu \to \infty$ which also corresponds to the case of isolated atoms (at least at the level of this schematic picture).

The metallic or insulating character of a material can thus be read off from the position of its Fermi energy with respect to bands and gaps. In a metal, ε_F lies in the midst of the valence band which is only partially filled. In an insulator, it lies in between occupied bands, in other words in the middle of a gap. Of course, these two cases are extremes and there exists a bunch of intermediate situations in which the Fermi energy lies closer or farther from the edge of the bands. And this proximity to the band edge correlates with the more or less metallic nature of the system. A relevant measure thus turns out to be the degree of filling of the band in which the Fermi energy lies.

1.2 Clusters between atom and bulk

Now that we have discussed a few basic properties of atoms and bonding in simple molecules and in bulk, we are coming to clusters as objects which establish a link between all these

cases. We try to work out their specificity and to explain why they are more than just large molecules or small pieces of bulk.

1.2.1 Clusters as scalable finite objects

Clusters are, by definition, aggregates of atoms or molecules with regular and arbitrarily scalable repetition of a basic building block. Their size is intermediate between atoms and bulk. One could thus loosely characterize them with a formula of the form X_n ($3 \lesssim n \lesssim 10^{5-7}$). The actual upper limit in size is hard to fix. As we shall see below, the definition of bulk may vary from one observable to another, namely a given physical property may reach its bulk value for a size different from another observable.

1.2.1.1 Clusters are more than molecules

Molecules usually have a well defined composition and structure. Think, e.g., of the well known molecules such as C_6H_6. Such systems have only a small number of isomers, a few units at most, even if they are themselves not small molecules. This is different for clusters, which often possess a large number of energetically close isomers and in which the number of isomers grows huge with increasing cluster size. For example, in such a small cluster as Ar_{13}, one has found hundreds of isomers, the actual number slightly depending on the detail of the interatomic potential used in the calculations, while less than 10 isomers were identified in Ar_8 [DJB87]. Another example are metal clusters which are also swamped by isomers, because of the softness of the binding.

When facing such a huge number of isomers, it is obvious that it is very hard to simply assess which is the most stable structure. This holds the more so as clusters are formed at finite temperature where it may be a delicate task to precisely tune the actual temperature of the formed clusters (see Section 2.1). Such a finite temperature allows a given cluster to explore a huge variety of isomers (=shapes), by simple thermal activation. And this process is all the more important as the number of accessible isomers is large. Stated in another, more technical, way, the potential energy surface (Born-Oppenheimer surface as discussed in Section 3.4.2) is very flat and this makes it very hard to figure out the actual ground-state structure of the system. Standard quantum chemistry techniques, well adapted to molecules with few isomers, are here often at a loss. Note finally that the difficulty in identifying the actual ground state structure constitutes an example of a more general feature, namely that many cluster properties do strongly depend on cluster size, see e.g. the example of shapes in Section 4.1.3.

1.2.1.2 Clusters are more than finite pieces of bulk

There are several features which distinguish a small piece of bulk from bulk [Ber98]. The basic difference between bulk and clusters can be seen from the level structure. Finite systems are basically characterized by discrete levels, at least in the low energy part of their spectrum. As is well known (see also Section 1.1.3.2), single-electron spectra in solids come along in bands each containing a continuum of levels. Passing from a discrete to a continuous set of levels is, in fact, also a continuous process. We have seen in Section 1.1.2.3 that the binding

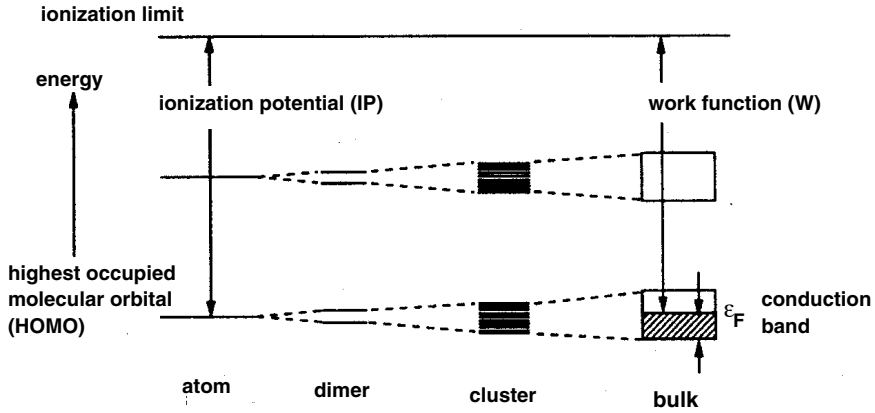

Figure 1.10: Schematic evolution of single-electron spectra in sodium clusters. After [KV93].

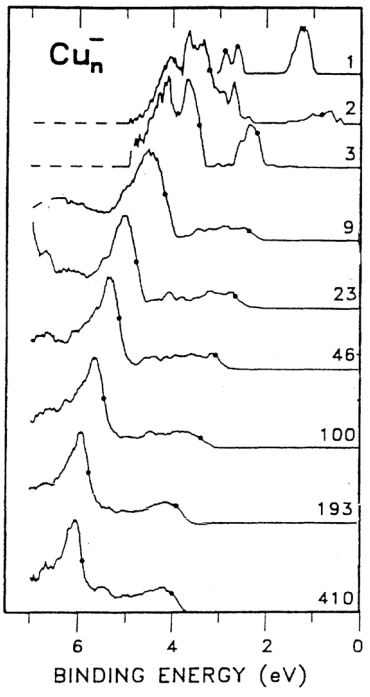

Figure 1.11: Evolution of single-electron spectra with system size for a series of Cu_n^- cluster anions with increasing size. The spectra are deduced from photo-electron spectroscopy. The upper atomic level is the $4s$ state and the lower one the $3d$, see also Figure 3.2. One can track down how the corresponding bands develop out of the atomic states. The points in the spectra for larger clusters indicate the upper band edge. After [CTCS90].

of two atoms, each bringing one electronic level, gives rise to two separate electronic levels (bonding and antibonding states). When more atoms are brought together, this splitting process continues and produces more and more levels which turn out to be closer and closer to each other, the larger the number of involved atoms. There is a thus a continuous path between a fully discrete molecular level scheme and a continuous (although with occasional gaps) level

Table 1.3: Schematic classification of clusters according to the number N of atoms. As a complement the diameter d for Na clusters is given (second row), together with an estimate of the ratio of surface to volume atoms f (surface fraction, in third row). After [KV93].

Observable	Very small clusters	Small clusters	Large clusters
Number of atoms N	$2 \leq N \leq 20$	$20 \leq N \leq 500$	$500 \leq N \leq 10^7$
Diameter d	$d \leq 1$ nm	1 nm$\leq d \leq 3$ nm	3 nm $\leq d \leq 100$ nm
Surface fraction f	undefined	$0.9 \gtrsim f \gtrsim 0.5$	$f \leq 0.5$

scheme in bulk. Such a path is illustrated in Figures 1.10 and 1.11. Figure 1.10 provides a schematic picture of this complexification starting from a simple dimer system (here Na_2) and going towards larger and larger clusters. The second figure (Figure 1.11) shows the evolution of experimental single electron spectra in Cu cluster anions. The figure nicely shows the evolution from atomic discrete levels to band-like pattern for heavier clusters. The levels had been recorded experimentally by photo-electron spectroscopy [CTCS90] (for photo-electron spectroscopy see also Figure 5.1 and Sections 2.2.3 and 2.3.8 as well as 5.2.3).

Another aspect where clusters are distinguished from bulk (and from molecules) are finite size effects in terms of surface to volume ratio. These features are much simpler to quantify than details of level structure. Most clusters are large enough such that one can speak about a surface zone. On the other hand, they are sufficiently small such that a sizeable fraction of the constituents lie on the surface of the system, while this is not true in bulk. Let us take as example the Ar_{55} cluster. It has 32 atoms on its surface. Now consider a piece of bulk material of 1 mm^3 volume. Taking an order of magnitude for the bond of 1 Åtells us that there are about $(10^{-3}/10^{-10})^3 \sim 10^{18}$ atoms in the sample, out of which about $(10^{18})^{2/3} \sim 10^{12}$ lie on the surface of the system. The ratio of surface atoms to total is thus $32/55 \sim 0.6$ in Ar_{55} as compared to about 10^{-6} in the bulk sample. Even taking a smaller sample of micrometer size the ratio would only increase to about 10^{-4}. There is thus a huge difference in the fraction of surface atoms when passing from clusters to bulk. And it turns out that this ratio constitutes a simple and efficient way to classify clusters. For an example see Figure 4.13.

1.2.1.3 Small and large clusters

As is obvious from the above discussion, clusters interpolate between atoms/molecules and bulk. But they are more than just trivial emanations of these two extremes cases. Of course, very small clusters look like molecules, though, and can thus be studied with chemistry methods, while very large clusters can be attacked with techniques stemming from solid state physics. In between, more specific techniques have to be developed for accessing clusters, as we shall see in this book. Already here, we can note that size is obviously a key parameter in cluster physics. Following the argument developed just above, a classification in terms of size can be given by considering the fraction of surface atoms to volume. Results are summarized in Table 1.3. Of course, this classification is schematic, and there is no strict boundary between the various classes of clusters. But it serves to sort the sizes and to give meaning to the terms small or large clusters in the following.

The question of size effects will be recurrent throughout this book, first, because clusters interpolate between atom and bulk with largely variable size, and second, because it turns out that most cluster properties do indeed strongly depend on size. But as already stressed above, convergence towards the bulk value with increasing cluster size essentially depends on the nature of the observable and on the resolution with which one looks at it. The best explanation is to consider a few examples. The experimental resolution of photo-electron spectra puts the transition from well separated discrete electron levels to quasi-continuous bands at about $N \approx 100$. Electronic shell effects, as e.g. magic HOMO-LUMO gaps, shrink $\propto N^{-1/3}$. And yet, their importance has triggered large efforts to resolve these up to the range of $N \approx 3000$, see Section 4.2.1.1. Atomic shell effects have been resolved up to $N \approx 10000$, see Section 4.2.1.2. The peak frequency of optical response converges also towards its bulk value with a term linear in $N^{-1/3}$. This means that colors keep drifting with size up to very large clusters in the range > 10000, see Figure 1.17 in Section 1.3.3.2. The cluster radius reaches the wavelength of visible light typically around $N \approx 10^9$, while the treatment of photo-excitation in the limit of long wavelengths is to be questioned much earlier. Many other examples will be found in this book.

1.2.2 Varying cluster material

There are, of course, various types of clusters in terms of bonding, depending on the nature of the atoms entering the cluster. As we have seen above, simple molecules as well as bulk can be grouped into the same four classes of bonds: metallic, covalent, ionic, and van-der-Waals bonding. It is natural then to classify bonding in clusters according to these four classes. And this turns out to constitute an important and relevant means for the classification of clusters. It also reflects deeper physical processes, even if these processes may sometimes differ from the ones observed either in molecules or in the bulk. The case of metalicity and its definition in terms of electron delocalization is a typical example of such a much debated criterion.

The first figure of this book, namely Figure 1.1, shows the famous C_{60} fullerene which provides a beautiful example of covalent bonding in clusters. In that case the cluster exhibits a well defined structure with electrons localized along the various links between the atoms. As expected, and as observed, other clusters made out of atoms of the carbon group exhibit covalent bonding as well, consider e.g., the case of the silicon clusters [Sug98].

Van-der-Waals binding prevails in rare-gas clusters, as e.g. for Ar. Figure 1.12 shows the geometry of Ar_{561}. This cluster corresponds to a closed atomic shell (see Section 4.2.1). The material keeps the electrons tightly bound to each mother atom. One can describe the system by effective atom–atom potentials (see Section 3.4.5.4) which are fairly simple to use. The structure in the figure has been computed with such an approach. Similar calculations have been extensively performed, because of the simplicity of the interatomic potential. There exist also many dynamical studies using molecular dynamics simulations of such rare-gas clusters, for example to study temperature effects [DJB87, JBB86].

Clusters with ionic bonding have been in the focus of many studies over a few years, in particular in view of potential applications in photography (e.g. AgBr clusters). The example shown in Figure 1.13 corresponds to a structurally simpler case, as it associates “ideal” partners (alkaline + halogen) in an almost stoichiometric manner. In such Na_nF_{n-1} structures, one Na electron is left “free” without a hosting F atom. It has thus to find a proper location in

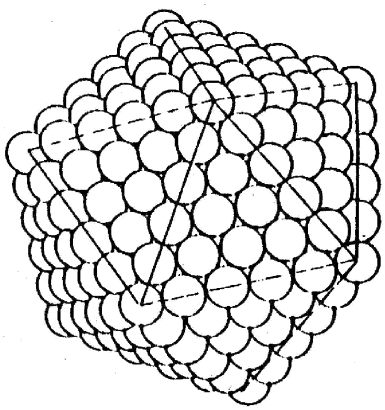

Figure 1.12: Geometrical configuration of the Ar_{561} cluster computed by simulated annealing (Section 3.4.3.2 and Appendix H.3) with effective atom–atom potentials. After [Hab94].

the cluster. Systematic studies in Na_nF_{n-1} clusters have shown that there basically exist four types of ionic structures corresponding to four different localizations of the excess electron provided by the excess Na atom. As illustrated in Figure 1.13, the regular NaF ionic structure clearly shines through, whatever the detail of the arrangement and the location of the excess electron. This regular ionic structure already appears in very small clusters such as Na_5F_4. In that particular case the excess electron remains localized around the "isolated" sodium atom, but there are other cases in which the electron may spread over a larger fraction of the structure such as for example in $Na_{14}F_{13}$.

The last class of clusters is made out of atoms which exhibit metallic bonding. The simplest example is here the case of alkaline atoms for which the metallic behavior is well assessed and simple to work out. Figure 1.14 shows the Na_4 cluster. It has a planar geometry which makes plotting and viewing simpler. Both electron density and ionic positions are explicitly represented. As expected in a metallic system, the electronic density extends more or less smoothly over the whole system. The small Na_4 cluster exhibits a clearly oblate shape. Correlatively, the electron cloud is strongly oblate, with a shape very similar to the ionic shape. The shape is determined here by electronic shell structure as discussed in Section 4.2.2.2. Larger metal clusters tend to favor spherical shapes due to the surface tension of the electron cloud. Crystalline shapes may emerge at very low temperature and/or for non-simple metals [Mar93]. In any case, the electrons have a large mobility and behave almost like an electron gas in a (spherical) container. Large metal clusters thus provide an ideal basis for the realization of the old Mie idea on the optical response of metallic spheres. This will be outlined below in Section 1.3.3. But before focusing on optical response of metal clusters let us briefly summarize our conclusions on the different types of binding.

A summary of the four classes of bonding and some of their consequences for cluster properties is presented in Table 1.4. It continues the energetic considerations of Section 1.1.2.4 on the dimer molecules. We recall the word of caution from Section 1.1 that such sorting schemes rely on idealizations and that reality falls often in between the categories. With that in mind, we can benefit from the table. We see that the least bound clusters are van-der-Waals (or molecular) clusters. They can be considered as a collection of weakly interacting atoms. The

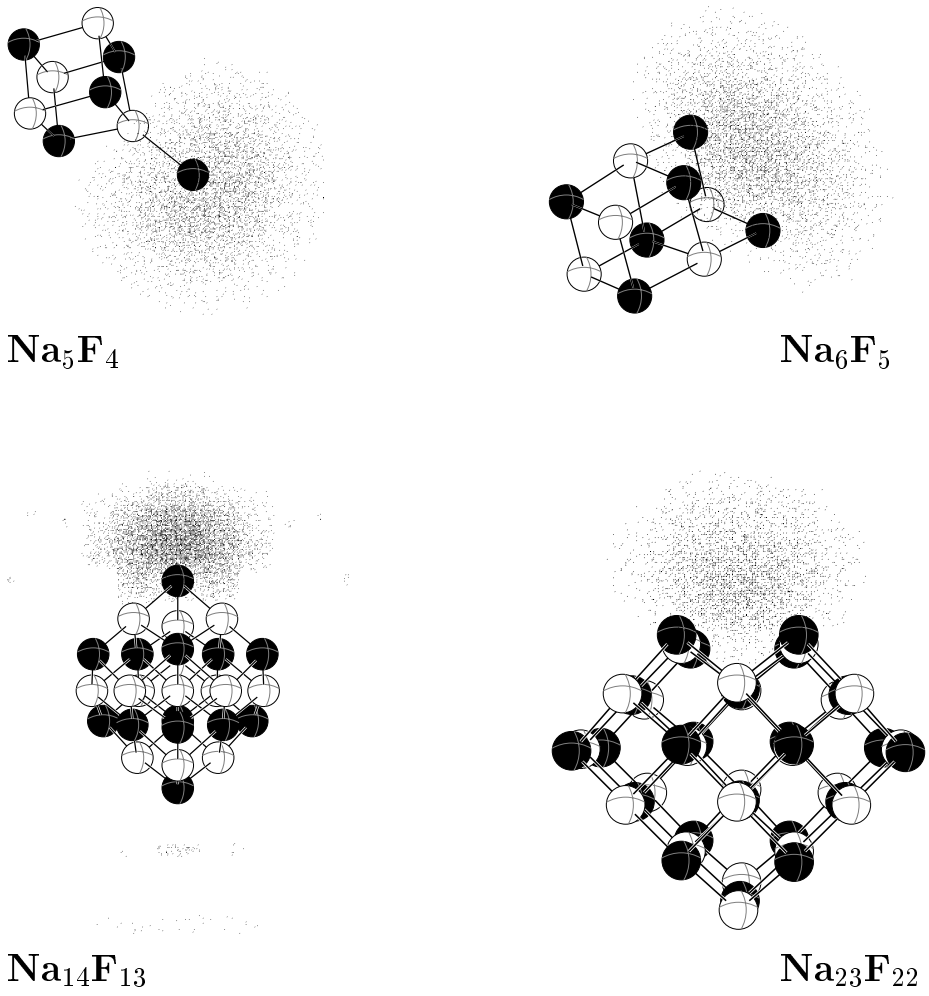

Figure 1.13: Typical structures of small Na_nF_{n-1} clusters. Na atoms are denoted by black spheres, F atoms by white spheres. Dots represent the electronic cloud. Note that there is only one "free" electron in all these clusters. Note also the various localizations of the electron depending on the numbers of Na and F atoms. For details see text. After [DGGM$^+$99].

strongest binding, on the contrary, usually appears in ionic clusters, although covalent clusters may bind almost as strongly. Metal clusters are generally a bit softer than covalent ones. They thus constitute an intermediate class between the almost unbound molecular clusters and the tightly bound ionic (or covalent) clusters.

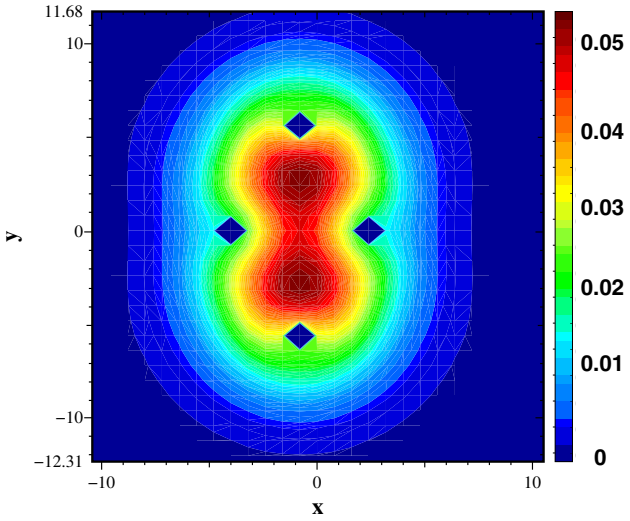

Figure 1.14: Equidensity plot of the electronic density of Na_4 computed with LDA (see Section 3.3.3). Plotted is the density in the x-y plane integrated over all z. The ionic positions are marked by small diamonds. The x and y scales are in units of a_0.

Table 1.4: Classification of binding in clusters. For each one of the four types of binding, examples of clusters (second column), the nature (third column) and typical binding energies (last column) are given. After [Hab94].

Type	Examples	Nature of binding	Binding energy
Ionic clusters	$(NaCl)_n$, Na_nF_{n-1}...	Ionic bonds	
		Strong binding	$\sim 2-4$ eV
Covalent clusters	C_{60}, S_n ...	Covalent bonding	
		Strong binding	$\sim 1-4$ eV
Metal clusters	Na_n, Al_n, Ag_n ...	Metallic bond	
		Moderate to strong binding	$\sim 0.5-3$ eV
van der Waals	Rare gas clusters	Polarization effects	
	Ar_n, Xe_n, ...	Weak binding	$\lesssim 0.3$ eV

Whatever cluster type, we see that binding energies lie in the eV range. Elementary bond lengths typically take values of a few a_0. Both these quantities thus fix the range of energies and distances characteristic of cluster physics. As complementing information, it is also interesting to evaluate a typical force in a cluster, in order to compare it to the intensity of an external field probing the system (laser or colliding projectile). Let us consider metal clusters, which exhibit a binding of intermediate strength. We take the example of a small alkaline cluster, Na_9^+, which we shall often use later on in applications. Its radius is of the order $R \sim 8a_0$

and we can estimate the typical electric field at surface as $E_0 \sim e^2/R^2 \sim 3.4\,\mathrm{eV/a_0}$. Such an electric field corresponds to a laser intensity $I \approx 10^{13-14}\mathrm{W/cm^{-2}}$ (Section 4.1.1.1). That means that non-destructive analysis of clusters by light has to be performed with laser intensities much below this value. In turn, with laser intensities of that order or larger, one will most probably destroy the cluster. For a more detailed view see Figure 3.3.

1.3 Metal clusters

1.3.1 Some specific properties

Metal clusters play a particularly pronounced role in cluster physics. They have attracted many investigators and the number of publications on that topic stays above average as compared to other materials. They will also appear quite often as examples throughout this book. This importance of metals is not the sole privilege of cluster physics. Following the introductory remarks of a famous book in solid state physics [AM76], one may recall that nature seems to have a "preference" for metals. More than two thirds of the elements are indeed metals. Furthermore, the understanding of metallic behavior turns out to constitute a key issue to understand the properties of solids, both conductors and insulators. Finally, as already pointed out before, the characteristic scalability of clusters finds particularly nice applications in the case of metal clusters. Electrons do form there a quasi free gas with generic properties, which lead to reasonably well understood behaviors with respect to size.

The features which make metals so different is the long mean free path of the valence electrons and the low melting point, ideally realized in alkalines and here at its best for Na. The nearly free propagation of the electrons throughout the cluster constitutes a generic test laboratory for the physics of an electron cloud, to be more precise, for a finite many-fermion system in the degenerate regime. The ionic background serves to deliver the finite bounds. Details of ionic structure can be easily wiped out, if necessary, by handling the cluster above the melting point. In other words, metal clusters are a near to perfect realization of a quantum system with self-adjusting bounds and shapes. One prominent consequence of the mobile electron cloud is a strong coupling to light with pronounced resonant behavior, the well known Mie surface plasmon resonance. We shall come back to this point at many places in this book. A first discussion in very simple terms is given in Section 1.3.3. The quantum mechanics of a confined electron cloud is dominated by shell effects. Metal clusters with their arbitrarily scalable size have provided here for the first time a laboratory to detect quantum mechanical shell effects up to system sizes of several thousands of fermions and with it shell beating and super-shells, see Section 4.2.1.1. The self-adjusting shape, as opposed to the fixed shapes of a quantum dot in a substrate, also delivers brilliant examples for the Jahn-Teller effect, as will be discussed in Section 4.2.2.2.

For pedagogical reasons we will thus use at many places throughout this book results obtained with metal clusters. This is motivated by two reasons. First, it does reflect the relative importance of metal clusters in experimental and theoretical investigations. Second, referring to the same test case at different places makes the links between the various approaches and applications more transparent. This makes the whole presentation more coherent and self contained. This can be seen, e.g., with respect to time scales. They will obviously play a

	Li	Na	K	Rb	Cs
r_s [a_0]	3.3	4.0	4.9	5.2	5.6
$\varepsilon_{\rm F}$ [eV]	4.7	3.2	2.1	1.9	1.6
$\frac{r_s}{v_{\rm F}}$ [fs]	0.13	0.20	0.30	0.35	0.40

Table 1.5: Gross properties of alkaline systems: Wigner Seitz radius r_s, Fermi energy ε_F and microscopic time scale r_s/v_F.

central role in the discussions of cluster dynamics. It is thus useful to have one case where one exemplifies in detail the various competing times. We will do this for alkaline metals.

1.3.2 On time scales

Before discussing the various time scales, we recall in table 1.5 the basic bulk parameters of alkaline metals. The different alkalines have the same order of magnitude within each observable. Changes stay within a factor of 2 to 3 and have monotonous trends with element number. The bulk parameters serve as "natural units" of length, energy and time. We will see that all electronic properties of alkaline clusters are about the same when expressed in terms of these natural units. The case is obvious for lengths where the Wigner-Seitz radius r_s sets the scale. For energies, we chose the Fermi energy $\varepsilon_{\rm F}$ which is related to the basic material parameters in a simple Fermi gas picture as (see also Appendix F.1)

$$\varepsilon_{\rm F} = \frac{\hbar^2}{2m}k_F^2 = \frac{\hbar^2}{2m}(\frac{9\pi}{4})^{2/3}\frac{1}{r_s^2} \quad . \tag{1.15}$$

The Fermi momentum $k_F = mv_F/\hbar$ of the system is directly linked to the Wigner Seitz radius of the material through the density $\rho = 3/(4\pi r_s^3) = k_F^3/(3\pi^2)$. The unit for time is chosen as r_s/v_F which is the time in which an electron at the Fermi surface travels through a distance r_s. The Fermi velocity can be deduced from the Fermi momentum and simply reads

$$v_F = \frac{\hbar}{m}k_F = \frac{\hbar}{m}(\frac{9\pi}{4})^{1/3}\frac{1}{r_s} \tag{1.16}$$

which fully defines our time unit in terms of r_s.

Various dynamical processes compete in metal clusters, both from the electronic and from the ionic side. A summary of typical time scales is given in Figure 1.15. Let us first concentrate on electrons. A key time scale is set by the all dominating Mie surface plasmon oscillations, in which the electron cloud collectively oscillates with respect to the ionic background (see Section 1.3.3). These collective oscillations do not last forever and the electronic motion loses sooner or later its collectivity due to coupling to detailed single-particle motion. This is partially Landau damping (as it is called in plasma physics [LP88], see also Section 4.3.5.1) and partially direct electron emission. The time scale for both processes is about the same and indicated by "s.p. times" in the figure. This initial damping generates "turbulence" in the electron cloud which, in turn, activates electron–electron collisions, which adds further damping and associated internal heating. The thermal energy of the electron cloud can then be transferred to ionic thermalization or released much later in terms of electron evaporation. The excited electron cloud also shakes the ions which react, of course, somewhat slower due to

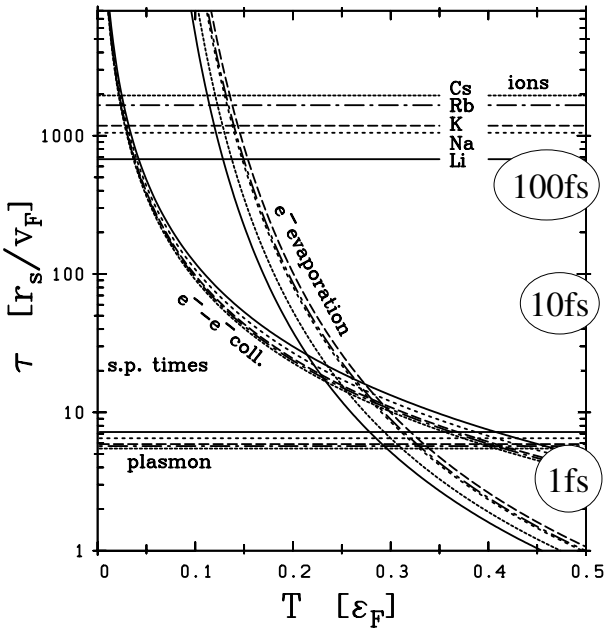

Figure 1.15: Time scales for alkaline clusters drawn versus internal excitation in terms of temperature T. Times and energies are expressed in natural units of each material according to Table 1.5. Orders of magnitude of the times in fs are also indicated for completeness on the right part of the figure.

their comparatively large mass. A typical time scale is here set by the cycle of ionic vibrations. First effects of ionic motion can already be spotted during the first quarter cycle. Subsequent ionic processes like fragmentation or monomer evaporation usually take much longer (several ionic cycles) but become faster with increasing violence of the excitation, as for example in a Coulomb explosion (see Section 5.5).

The times scales change with the internal state of the cluster. In Figure 1.15 we use temperature as a simple indicator of the excitation regime (keeping in mind that times may depend on the particular excitation mechanism in the early, transient stages of a dynamical process). Temperature has the additional advantage that it is an intensive quantity, independent of system size (unlike an extensive quantity as the internal excitation energy). Figure 1.15 thus shows the various time scales as a function of temperature. Again, we take the Fermi energy ε_F as a unit for temperatures (the Boltzmann constant k is set to one here). The trends are much different from one time to another. That means the relation between times changes dramatically with the energy of the excitation. For example, electron evaporation is an extremely slow process for low excitations. But it becomes competitive with other electronic mechanisms at high excitations. Electron–electron collisions also depend strongly on temperature and are unimportant for low excitations. The plasmon and single-particle cycles, on the other hand, stay rather robust.

Figure 1.15 also demonstrates that all electronic time scales from the different materials gather close together when expressed in the natural units of the electron cloud. The ionic time scales, on the other hand, are dominated by the independent parameter of ionic mass and thus show a larger spread amongst the materials. But ionic time scales group themselves in a time range well separated from basic electronic scales, as expected in view of the large mass difference between ions and electrons.

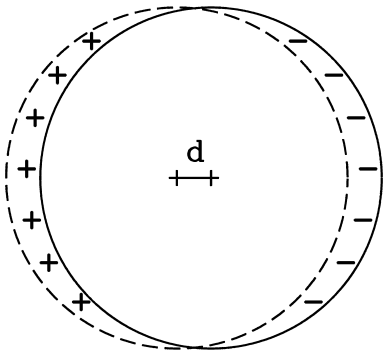

Figure 1.16: Schematic representation of Mie surface plasmon. The electrons (represented by a negatively charged spherical cloud) are collectively displaced with respect to the ionic background (represented by a positively charged sphere). Inside most of the system, the original neutrality of the system is preserved. Net charges only appear on the surface of the system, a positive one on one side and a corresponding negative one on the opposite side.

In a dynamical context, the internal time scales of a cluster are to be complemented by the time scale of the excitation processes. Nanosecond lasers are beyond any time shown in Figure 1.15. That is a regime where the frequency hence plays the dominant role. Collisions with highly charged and fast ions may be below any time scale shown (typically in the fs or sub-fs range). Fast ions thus cover the opposite regime where frequencies are unimportant and only forces count, a domain which is also explored by intense laser beams (here for simple reasons of power). Slower ions may be associated with time scales of tens of fs or even more. Similarly, femtosecond (fs) lasers have just the time scales which interfere with the various time scales of metal clusters. It is obvious that this gives rise to a huge variety of accessible dynamical processes which can be triggered by fs laser experiments. We shall come back to these various excitation processes on many occurrences in this book.

1.3.3 Optical properties

1.3.3.1 The simple Mie picture

As suggested in Section 1.2.2, metal clusters can be viewed as metallic spheres filled with an almost uniform electron gas not too tightly bound to the ionic background. No surprise that a moderate external electric field may easily affect such clusters whose response then provides a fingerprint of crucial cluster properties. This is just the essence of Mie theory of response of a metallic sphere to light [Mie08], for extensive explanations see e.g. [KV93]. Let us briefly outline this simple but generic picture.

We start with an oversimplified model of a spherical metal cluster X_N. The ionic background is represented by a homogeneous positively charged sphere with radius R and density ρ. Electrons are associated to a negatively charged sphere with the same density ρ such that the total system is neutral in its ground state. For the sake of simplicity, we shall furthermore assume that both electrons and ions move as rigid spheres against each other. In fact, as long as the system is not too much perturbed, electrons do indeed primarily respond in a collective and almost rigid way. Let us now assume that a small uniform external electric field $\mathbf{E}_{\rm ext}$ is applied to this system. The net effect of $\mathbf{E}_{\rm ext}$ is to separate slightly electrons from ions. Because ions are much heavier than electrons, they basically remain fixed and the electrons are displaced with respect to ions, as illustrated in Figure 1.16. The separation builds up a strong Coulomb attraction between ions and electrons which provides a restoring force on the

displaced electron cloud counteracting $e\mathbf{E}_{\rm ext}$. Denoting by $\mathbf{d}$ the actual separation of ionic and electronic center of masses the net force acting on the electron cloud (along the direction of $\mathbf{E}_{\rm ext}$) reads for small $\mathbf{d}$

$$\mathbf{F} = -N\frac{4\pi\rho e^2}{3}\mathbf{d} = N\mathbf{E}_{\rm ext} \quad . \tag{1.17}$$

Once the external perturbation is switched off, there only remains the attractive force between electrons and ions. This force is proportional to the actual separation d between ions and electrons. The mobile part of the system is the electron cloud having total mass $Nm_{\rm el}$. It will thus undergo harmonic oscillations around ions, with a frequency

$$\omega_{\rm Mie}^2 = \frac{4\pi\rho e^2}{3m_{\rm el}} = \frac{e^2}{m_{\rm el}r_s^3} \tag{1.18}$$

where $m_{\rm el}$ is the electron mass. This oscillation frequency is known as the Mie frequency.

When a cluster is irradiated by light the situation is about the same as described above. Optical wavelengths range in the micrometer domain, which is much larger than most cluster sizes. The electrical field is thus locally uniform at the cluster site and provokes the above described collective oscillation of the electron cloud against the ionic background. The typical values of $\omega_{\rm Mie}$ for simple alkaline metals lie in the visible part of the electromagnetic spectrum, whence the term "optical response" to characterize this phenomenon. For the alkalines, whose r_s were given in table 1.5, the Mie frequencies are: $\hbar\omega_{\rm Mie}({\rm Li}) = 4.5$ eV, $\hbar\omega_{\rm Mie}({\rm Na}) = 3.4$ eV, $\hbar\omega_{\rm Mie}({\rm K}) = 2.5$ eV, $\hbar\omega_{\rm Mie}({\rm Rb}) = 2.3$ eV, and $\hbar\omega_{\rm Mie}({\rm Cs}) = 2.1$ eV. These estimates fit fairly well with experimental values as we will see later. The relations are more involved for non-simple metals as, e.g., noble metals. There one needs to take the polarizability of the core electrons into account (see Section 1.3.3.2 and the discussion in Section 4.3.4.1).

1.3.3.2 The dielectric picture

The explicit picture of an oscillating electron cloud led to the expression (1.18) of the Mie frequency simply in terms of bulk density ρ. In more involved materials one needs to account for internal polarizability. This can be done at the level of macroscopic models by employing the bulk dielectric constant of the medium ϵ. Note that dielectric media require one to make a distinction between an externally applied electrical field $\mathbf{E}_{\rm ext}$ and the effective internal field $\mathbf{E}_{\rm int}$ which emerges when cumulating the additional fields from internal polarization effects. The external field is directly related to the external sources while the internal field describes the net effect on moving charges, accounting for both external sources and induced charges. Both are related at a macroscopic level through the standard relation

$$\mathbf{E}_{\rm int}(\mathbf{r},\omega) = \epsilon(\mathbf{r},\omega)\mathbf{E}_{\rm ext}(\mathbf{r},\omega) \quad . \tag{1.19}$$

This relation is given for the dynamical polarizability $\epsilon(\mathbf{r},\omega)$ which is more easily formulated in terms of frequency ω of the applied field. Transformation to the time domain yields a polarizability with memory kernel depending on all past times. The space dependence can be

omitted in homogeneous materials. But it plays a crucial role at interfaces between different materials.

Clusters are finite systems with a large surface area. Let us thus consider a finite piece, namely a spherical sampling, of the bulk material with given dielectricity ϵ. The response of that dielectric sphere to a homogeneous external electrical field can be worked out with standard techniques of electro-dynamics (see e.g. [Jac62, KV93]). The result for this spherically symmetric system is

$$\mathbf{E}_{\rm int} = \frac{3}{2+\epsilon}\mathbf{E}_{\rm ext} \quad . \tag{1.20}$$

The Mie resonance frequency is found at the point where the internal field becomes self-supporting, i.e. where we can have a finite $\mathbf{E}_{\rm int}$ for zero excitation $\mathbf{E}_{ext}$. This defines the resonance frequency $\omega_{\rm Mie}$ through

$$2 + \epsilon(\omega_{\rm Mie}) = 0 \quad . \tag{1.21}$$

That definition holds for a much broader class of metals than the simpler relation (1.18). The price is that one has to know the whole bulk $\epsilon(\omega)$.

In the following, we want to show that the definition (1.21) becomes identical with (1.18) for the case of simple metals. To that end, we have first to develop a simple model for the bulk dielectric constant. Let us thus consider an "infinite" piece of metal irradiated by an external light source. The external electric field polarizes the medium. The effect can be estimated at an elementary level by considering the motion of a single electron subject to the net electric field $\mathbf{E}_{\rm int}$. The electron follows the Newtonian equation of motion

$$m\frac{d^2\mathbf{r}}{dt^2} = -e\mathbf{E}_{\rm int} \quad . \tag{1.22}$$

For a sinusoidal electric field of frequency ω, the solution is also sinusoidal with the same frequency. The polarization of the medium then simply reads

$$\mathbf{P} = -\rho e\mathbf{r} = -\frac{\rho e^2}{m\omega^2}\mathbf{E}_{\rm int} \tag{1.23}$$

from which one deduces the total field $\mathbf{E}_{\rm int} = \mathbf{E}_{ext} + \mathbf{P} = \epsilon\mathbf{E}_{ext}$ and the frequency dependent dielectric function

$$\epsilon(\omega) = 1 - \frac{\omega_{\rm p}^2}{\omega^2} \quad , \quad \omega_{\rm p} = \sqrt{\frac{4\pi\rho e^2}{m_{\rm el}}} = \sqrt{\frac{3e^2}{m_{\rm el}r_s^3}} \tag{1.24}$$

where $\omega_{\rm p}$ is the bulk plasma frequency of the medium. The plasma frequency is related to $\epsilon = 0$. It characterizes the point of infinite response in bulk, i.e. an eigenmode of bulk oscillations. The infinite response never occurs in practice. Damping processes take over far before the amplitude explodes. The damping can be taken into account by introducing one relaxation time τ at the present level of estimate. This generalizes the above dielectric response to the Drude model [AM76], giving $\epsilon = 1 - \omega_{\rm p}^2\tau/(\omega(\imath + \omega\tau))$ which merges into the form Eq. (1.24) for the limit $\tau \longrightarrow \infty$.

Let us now insert the dielectric function Eq. (1.24) into the condition Eq. (1.21) for a Mie plasmon. This yields with a bit of simple algebra $\omega_{\rm Mie} = \omega_{\rm p}/\sqrt{3}$ and thus precisely the frequency (1.18). This bulk-oriented approach thus allows one to recover the simple relation for the Mie frequency when using a spherical dielectric. The macroscopic treatment can easily be extended to more general shapes as, e.g., spheroidal clusters and allows one here to sort a lot of global phenomena. This line is followed to a large extend in [KV93]. In this book, however, we will put more weight on the microscopic treatment as outlined in Chapter 3.

As is clear from the above discussion, in a finite system electron oscillations will dominantly show up at the surface of the system, while in bulk they manifest themselves through electron density oscillations at plasma frequency $\omega_{\rm p}$, independent from the surface. In fact both mechanisms do exist in finite systems like clusters. In other words, an electric field induces both electron displacement *and* electron density fluctuations. It simply turns out that in a finite system the surface effect dominates over the bulk effect and one thus mostly observes the surface response, theoretically as well as experimentally. This means that photoabsorption spectra of the optical response of metal clusters to light are dominated by the surface plasmon, while a, usually much suppressed, contribution from the so called volume plasmon (corresponding to the bulk-like response) may be spotted in the frequency domain around $\sqrt{3}$ times the surface plasmon.

The existence of a resonance such as the Mie plasmon (or the volume plasmon) has important consequences on the way the system will actually couple to light. To make the point specific let us consider the case of a cluster subject to a laser irradiation, a situation that we shall encounter at many places along this book. In this case, one can easily estimate the amount of absorbed laser power by the system by simply considering the motion of individual electrons subject to the laser field of frequency $\omega_{\rm las}$ and the damped (with relaxation time τ) plasmon oscillations of frequency $\omega_{\rm Mie}$ (following, in that respect the simplest Drude model). The instantaneous absorbed power can be expressed as $\mathcal{P}_{\rm abs} = -e\rho\mathbf{v}\mathbf{E}$ averaged over all possible electron velocities $\mathbf{v}$. Time averaging over one laser cycle, one obtains the well known resonant absorption form

$$< \mathcal{P}_{\rm abs} >= \mathcal{P}_0 \frac{u^2}{(1-u^2)^2 + (u/\omega_{\rm Mie}\tau)^2} \tag{1.25}$$

where $u = \omega_{\rm las}/\omega_{\rm Mie}$. The above form obviously exhibits a resonance at $\omega_{\rm las}/\omega_{\rm Mie}$. This means that when irradiating a cluster with a laser field one should expect resonant energy absorption when the laser frequency comes close to the plasmon frequency. This resonant behavior will actually be observed and exploited in many situations all along this book (see in particular the discussion in Section 5.3.1.1).

1.3.3.3 Optical response in metal clusters

The Mie model and the dielectric approach, outlined above, show that metals resonantly couple to light, both in bulk as well as in small particles. In finite systems such as clusters, the surface plasmon dominates the response and we shall mostly focus on this aspect in the following. The resonance frequencies provided by the above models, Eqs. (1.18) or (1.24), are independent of cluster size. This does not fully agree with experimentally observed response spectra. Figure 1.17 shows optical absorption spectra of deposited clusters of various sizes.

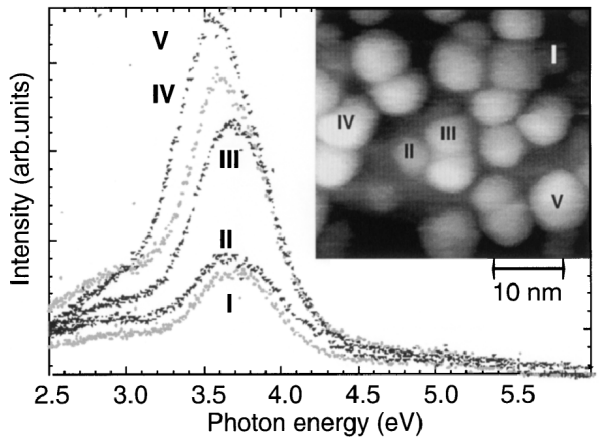

Figure 1.17: Photoemission spectra of Ag clusters of various sizes as indicated. The inset shows the corresponding STM image of the various clusters whose spectra have been recorded. Note the dependence of the peak response as a function of cluster size. From [NEF00].

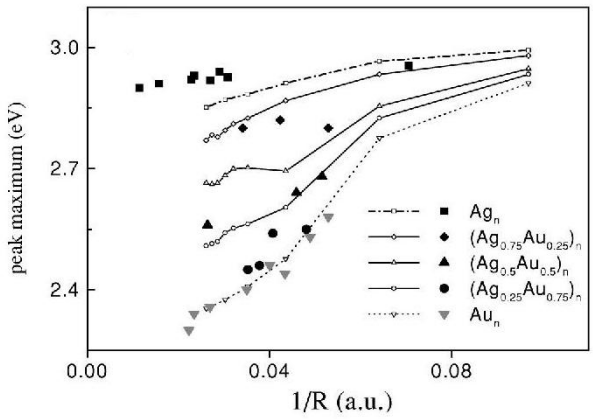

Figure 1.18: Resonance frequencies for embedded alloy clusters from Ag and Au with several degrees of mixing. The frequencies are drawn as a function of inverse cluster radius $1/R$. From [GLC+01].

The peak in the plasmon response shows a clear trend as a function of cluster size, which can be roughly estimated from the inset.

More systematic measurements of this effect have been reported in many occurrences. Figure 1.18 shows a systematics of results obtained for metal clusters embedded in a glass matrix. (Such clusters are typically the ones we discussed at the very beginning of this chapter, invoking Roman art and crafts.) The dependence of surface plasmon frequency on cluster radius R is clear. There is a weak linear trend with $1/R$. The bulk limit $1/R \to 0$ tends nicely towards Mie frequency when estimated according to Eq. (1.24) with the bulk dielectric constant. The slope of the trend depends obviously on the material, here on the different degrees of mixing in the alloy. Driving measurements to small clusters shows deviations from the linear trend through finite-size quantum effects. We shall come back in more detail to this point in Section 4.3.

1.4 Conclusion

Although clusters have been used for centuries, in particular by craftworkers and in photography, they have become the focus of dedicated scientific investigations only very recently, essentially during the last quarter of the twentieth century. This late interest is, to a large extent, related to the fact that one was not able to produce free clusters, until recently. But since interest in clusters has grown, investigations on these systems have led to major scientific achievements, the most famous being probably the discovery of fullerenes, with all the potential applications it unraveled, in terms of physics and chemistry of carbon at the nanometer scale.

As we have seen throughout this chapter, clusters are specific objects. They are neither big molecules nor finite pieces of bulk. One of their major characteristics is precisely their scalability, which allows them to constitute one almost unique case of systems truly interpolating between individual atom and bulk. This has obviously profound theoretical applications for the many body problem, an aspect which interestingly complements the potential technological applications mentioned just above in the case of Carbon.

In clusters atoms bind together to form the system itself in a way similar to what occurs in simple molecules or in bulk. Indeed, one observes the same different types of bonding, namely ionic, covalent, metallic and van der Waals bonding in clusters. This gives rise to four corresponding classes of clusters, with different binding characteristics, in particular in terms of the robustness of the such formed structures. Of course such a classification primarily provides a guide rather than a rigid classification. Clusters may even exhibit various types of bonding as a function of their size.

Among the four classes of clusters, metal clusters, in which electrons constitute a highly delocalized, quasi free, gas, play a particular role in the field. They have indeed been the focus of a particularly large number of investigations, which allow one to have systematics on several physical properties. They furthermore respond in a particularly simple and robust way to light in terms of the so called surface plasmon, an effect identified in the early twentieth century by G. Mie. This behavior again makes their manipulation, in particular by means of laser fields, especially simple. Metal clusters will thus be considered in a sizable fraction of the discussions in this book. This is particularly true in dynamical questions, which constitute a central topic of this book.